

Multi-index Importance Sampling for McKean-Vlasov Stochastic Differential Equation

Nadhir Ben Rached ^{*}, Abdul-Lateef Haji-Ali [†], Shyam Mohan Subbiah Pillai [‡]
and Raúl Tempone [§] [¶]

Abstract

This work introduces a novel approach that combines the multi-index Monte Carlo (MC) method with importance sampling (IS) to estimate rare event quantities expressed as an expectation of a smooth observable of solutions to a broad class of McKean-Vlasov stochastic differential equations. We extend the double loop Monte Carlo (DLMC) estimator, previously introduced in our works (Ben Rached et al., 2022a,b), to the multi-index setting. We formulate a new multi-index DLMC estimator and conduct a comprehensive cost-error analysis, leading to improved complexity results. To address rare events, an importance sampling scheme is applied using stochastic optimal control of the single level DLMC estimator. This combination of IS and multi-index DLMC not only reduces computational complexity by two orders but also significantly decreases the associated constant compared to vanilla MC. The effectiveness of the proposed multi-index DLMC estimator is demonstrated using the Kuramoto model from statistical physics. The results confirm a reduced complexity from $\mathcal{O}(\text{TOL}_r^{-4})$ for the single level DLMC estimator (Ben Rached et al., 2022a) to $\mathcal{O}(\text{TOL}_r^{-2}(\log \text{TOL}_r^{-1})^2)$ for the considered example, while ensuring accurate estimation of rare event quantities within the prescribed relative error tolerance TOL_r .

Keywords: McKean-Vlasov stochastic differential equation, importance sampling, multi-index Monte Carlo, decoupling approach, double loop Monte Carlo.

2010 Mathematics Subject Classification 60H35. 65C30. 65C05. 65C35.

^{*}Department of Statistics, School of Mathematics, University of Leeds (N.BenRached@leeds.ac.uk).

[†]Department of Actuarial Mathematics and Statistics, School of Mathematical and Computer Sciences, Heriot-Watt University, Edinburgh, UK (A.HajiAli@hw.ac.uk).

[‡]Corresponding author; Chair of Mathematics for Uncertainty Quantification, Department of Mathematics, RWTH Aachen University, Aachen, Germany (subbiah@uq.rwth-aachen.de).

[§]Computer, Electrical and Mathematical Sciences & Engineering Division (CEMSE), King Abdullah University of Science and Technology (KAUST), Thuwal, Saudi Arabia (raul.tempone@kaust.edu.sa). Alexander von Humboldt Professor in Mathematics for Uncertainty Quantification, RWTH Aachen University, Aachen, Germany (tempone@uq.rwth-aachen.de).

[¶]This work was supported by the KAUST Office of Sponsored Research (OSR) under Award No. URF/1/2584-01-01 and the Alexander von Humboldt Foundation. This work was also partially performed as part of the Helmholtz School for Data Science in Life, Earth and Energy (HDS-LEE) and received funding from the Helmholtz Association of German Research Centres. For the purpose of open access, the author has applied a Creative Commons Attribution (CC BY) licence to any Author Accepted Manuscript version arising from this submission.

1 Introduction

McKean-Vlasov stochastic differential equations (MV-SDEs) are a special class of SDEs whose drift and diffusion coefficients depend on the law of the solution itself (McKean Jr, 1966). These equations arise from the mean-field behaviour of stochastic interacting particle systems, which find applications in various fields such as pedestrian modeling (Haji Ali, 2012), animal behavior studies (Erban and Haskovec, 2011), biology (Dobramysl et al., 2016), finance (Bush et al., 2011), and chemistry (Acebrón et al., 2005). Detailed analysis (Haji-Ali et al., 2021; Mishura and Veretennikov, 2020; Buckdahn et al., 2017; Crisan and McMurray, 2018) and numerical treatment (Haji-Ali and Tempone, 2018; dos Reis et al., 2022; Szpruch et al., 2019; Crisan and McMurray, 2019) of MV-SDEs can be found in the referenced works. In this work, our focus lies in estimating rare event quantities, which are expressed as expectations of observables associated with the solution to a broad class of MV-SDEs at a fixed terminal time T . Specifically, we develop a computationally efficient Monte Carlo (MC) estimator for $\mathbb{E}[G(X(T))]$, where $G : \mathbb{R}^d \rightarrow \mathbb{R}$ represents a sufficiently smooth rare event observable, and $X : [0, T] \times \Omega \rightarrow \mathbb{R}^d$ denotes the stochastic McKean-Vlasov process.

Stochastic P -particle systems are commonly employed to approximate MV-SDEs. These systems consist of P coupled d -dimensional Itô SDEs, and they exhibit a mean-field limit as the number of particles approaches infinity (Sznitman, 1991). Estimating expectations associated with particle systems by numerically solving the $(P \times d)$ -dimensional Kolmogorov backward equation quickly becomes computationally intractable. To address this challenge, Monte Carlo (MC) methods are used to obtain computationally feasible estimates. Previous works (Li et al., 2023; Haji-Ali and Tempone, 2018) have studied MC methods that utilize Euler-Maruyama time-discretized particle systems, assuming bounded, Lipschitz drift and diffusion coefficients, for smooth, non-rare observables. These methods achieve a complexity of $\mathcal{O}(\text{TOL}^{-4})$ for a prescribed error tolerance TOL. However, when it comes to rare events, MC methods become prohibitively expensive. This is due to the significant increase in the relative estimator complexity constant as the event becomes rarer (Kroese et al., 2013). To tackle this issue, importance sampling (IS) is employed as a variance reduction technique to mitigate the limitations of standard MC methods in the rare event regime (Kroese et al., 2013).

The initial study of importance sampling (IS) for rare events in the context of MV-SDEs was conducted in (dos Reis et al., 2023; Ben Rached et al., 2022a). In (dos Reis et al., 2023), the authors propose a decoupling approach that involves defining a decoupled MV-SDE. Here, they replace the McKean-Vlasov law in the drift/diffusion coefficients of the MV-SDE with an empirical realization of the law computed beforehand by running a particle system. Measure change for IS is performed on this decoupled process ensuring that IS is separated from the estimation of the McKean-Vlasov law. Building upon this decoupling approach, our previous work (Ben Rached et al., 2022a) introduces a double loop Monte Carlo (DLMC) estimator. Stochastic optimal control theory is then utilized to derive a zero-variance time- and pathwise-dependent IS control. Subsequently, we develop an adaptive DLMC algorithm with a complexity of $\mathcal{O}(\text{TOL}^{-4})$, matching that of the MC estimator for non-rare observables in (Haji-Ali and Tempone, 2018). In the subsequent work (Ben Rached et al., 2022b), we combine multilevel MC methods with the aforementioned IS scheme to

reduce the computational complexity of the estimator compared to the single-level estimator introduced in (Ben Rached et al., 2022a).

The multi-index Monte Carlo (MIMC) method was introduced in (Haji-Ali et al., 2016a) to tackle problems involving multiple (two or more) discretization parameters. This approach builds upon the efficiency of multilevel MC but requires mixed regularity with respect to the discretization parameters. While the multi-index method has been applied to smooth, non-rare observables associated with particle systems in (Haji-Ali and Tempone, 2018), our goal in this study is to combine the multi-index technique with the IS scheme introduced in (Ben Rached et al., 2022a). The objective is to develop an estimator for rare event expectations associated with MV-SDEs that is not only efficient but also surpasses the performance of the multilevel DLMC estimator (Ben Rached et al., 2022b). Although the combination of multilevel MC with importance sampling has been studied in various contexts (Ben Alaya et al., 2023; Kebaier and Lelong, 2018; Fang and Giles, 2019; Ben Hammouda et al., 2020) before, this work represents, to the best of our knowledge, the first attempt to integrate IS with multi-index MC. We summarize the main contributions of this paper as follows:

- This paper extends the DLMC estimator introduced in (Ben Rached et al., 2022a,b) to the multi-index setting and proposes a novel multi-index DLMC estimator for MV-SDEs. We include detailed discussion on the proposed estimator’s bias and variance, and devise a complexity theorem, showing improved complexity compared with multilevel DLMC. We also formulate a robust adaptive multi-index DLMC algorithm that iteratively determines optimal parameters.
- This paper proposes a novel combination of IS scheme with the multi-index DLMC estimator to handle rare event quantities. We apply the IS control developed for the DLMC estimator in (Ben Rached et al., 2022a) to all multi-indices in the multi-index DLMC estimator.
- This paper investigates numerically the effect of the IS scheme on the variance of this novel multi-index DLMC estimator. Numerical simulations confirm significant variance reduction due to this IS scheme, improving $\mathcal{O}(\text{TOL}_r^{-4})$ complexity, obtained in (Ben Rached et al., 2022a) for the considered example; to $\mathcal{O}(\text{TOL}_r^{-2}(\log \text{TOL}^{-1})^2)$ in the multi-index setting, while allowing feasible rare event quantity estimation up to the prescribed relative error tolerance TOL_r .

The paper is structured as follows. In Section 2, we provide an introduction to the MV-SDE, along with the associated notation and problem statement. Section 3 presents the decoupling approach for MV-SDEs (dos Reis et al., 2023) and formulates a DLMC estimator based on this approach. Moving on to Section 4, we present the zero-variance IS control for the decoupled MV-SDE, derived using stochastic optimal control techniques. Additionally, we introduce the DLMC estimator with IS from our previous work (Ben Rached et al., 2022a). In Section 5, we introduce the novel multi-index DLMC estimator and provide new complexity results for this estimator. We then propose an IS scheme for the multi-index DLMC estimator. Furthermore, we develop an adaptive multi-index DLMC algorithm, which enables the feasible estimation of rare event quantities associated with MV-SDEs.

To validate our approach and verify the assumptions made in this work, Section 6 applies the proposed methods to the Kuramoto model from statistical physics. We also provide numerical verification of the derived complexity rates for the multi-index DLMC estimator with respect to an appropriate rare event observable.

2 McKean-Vlasov Stochastic Differential Equation

We consider a broad class of McKean-Vlasov equations that arise from the mean-field limit of stochastic interacting particle systems with pairwise interaction kernels (Sznitman, 1991). Consider the probability space $\{\Omega, \mathcal{F}, \{\mathcal{F}_t\}_{t \geq 0}, P\}$, where \mathcal{F}_t is the filtration of a standard Wiener process $\{W(t) : t \in [0, T]\}$. For functions $b : \mathbb{R}^d \times \mathbb{R} \rightarrow \mathbb{R}^d$, $\sigma : \mathbb{R}^d \times \mathbb{R} \rightarrow \mathbb{R}^{d \times d}$, $\kappa_1 : \mathbb{R}^d \times \mathbb{R}^d \rightarrow \mathbb{R}$ and $\kappa_2 : \mathbb{R}^d \times \mathbb{R}^d \rightarrow \mathbb{R}$, consider the following Itô SDE for the McKean-Vlasov stochastic process $X : [0, T] \times \Omega \rightarrow \mathbb{R}^d$

$$\begin{cases} dX(t) = b\left(X(t), \int_{\mathbb{R}^d} \kappa_1(X(t), x) \mu_t(dx)\right) dt \\ \quad + \sigma\left(X(t), \int_{\mathbb{R}^d} \kappa_2(X(t), x) \mu_t(dx)\right) dW(t), \quad t > 0 \\ X(0) = x_0 \sim \mu_0 \in \mathcal{P}(\mathbb{R}^d), \end{cases} \quad (1)$$

where $W : [0, T] \times \Omega \rightarrow \mathbb{R}^d$ is a d -dimensional Wiener process with mutually independent components; $\mu_t \in \mathcal{P}(\mathbb{R}^d)$ is the mean-field law of $X(t)$, where $\mathcal{P}(\mathbb{R}^d)$ is the space of all probability measures in \mathbb{R}^d ; and $x_0 \in \mathbb{R}^d$ is a random initial state with distribution $\mu_0 \in \mathcal{P}(\mathbb{R}^d)$. Functions $b(\cdot)$ and $\sigma(\cdot)$ are called drift and diffusion functions/coefficients, respectively. Under certain smoothness and boundedness conditions on $b, \sigma, \kappa_1, \kappa_2$, one can prove existence and uniqueness of solutions to (1) (Haji-Ali et al., 2021; Mishura and Veretennikov, 2020; Crisan and Xiong, 2010; Sznitman, 1991; Hammersley et al., 2021). The distribution of the McKean-Vlasov process X satisfies the following Fokker-Planck partial differential equation (PDE),

$$\begin{cases} -\frac{\partial \mu(s, x; t, y)}{\partial s} - \sum_{i=1}^d \frac{\partial}{\partial x_i} \left(b_i\left(x, \int_{\mathbb{R}^d} \kappa_1(x, z) \mu(s, z; t, y) dz\right) \mu(s, x; t, y) \right) \\ \quad + \sum_{i=1}^d \sum_{j=1}^d \frac{1}{2} \frac{\partial^2}{\partial x_i \partial x_j} \left(\sum_{k=1}^d \sigma_{ik} \sigma_{jk} \left(x, \int_{\mathbb{R}^d} \kappa_2(x, z) \mu(s, z; t, y) dz \right) \right. \\ \quad \left. \mu(s, x; t, y) \right) = 0, \quad (s, x) \in (t, \infty) \times \mathbb{R}^d \\ \mu(t, x; t, y) = \delta_y(x), \end{cases} \quad (2)$$

where $\mu(s, x; t, y)$ denotes the conditional distribution of $X(s)$ given that $X(t) = y$; and $\delta_y(\cdot)$ denotes the Dirac measure at y . (2) is a non-linear integral differential PDE with non-local terms. The cost of numerical approximation of (2) up to relative error tolerances increases exponentially with the number of dimensions d , motivating study of strong approximations to (1).

Consider following system of P exchangeable Itô SDEs, also known as a stochastic interacting particle system, with pairwise interaction kernels comprising P particles (Sznitman, 1991). For $p = 1, \dots, P$, we have the following SDE for the process $X_p^P : [0, T] \times \Omega \rightarrow \mathbb{R}^d$,

$$\begin{cases} dX_p^P(t) = b \left(X_p^P(t), \frac{1}{P} \sum_{j=1}^P \kappa_1(X_p^P(t), X_j^P(t)) \right) dt \\ \quad + \sigma \left(X_p^P(t), \frac{1}{P} \sum_{j=1}^P \kappa_2(X_p^P(t), X_j^P(t)) \right) dW_p(t), \quad t > 0 \\ X_p^P(0) = (x_0)_p \sim \mu_0 \in \mathcal{P}(\mathbb{R}^d), \end{cases} \quad (3)$$

where $\{(x_0)_p\}_{p=1}^P$ are independent and identically distributed (iid) random variables sampled from the initial distribution μ_0 ; $\{W_p\}_{p=1}^P$ are mutually independent d -dimensional Wiener processes, also independent of $\{(x_0)_p\}_{p=1}^P$. Equation (3) approximates the mean-field law μ_t from (1) by an empirical law based on particles $\{X_p^P(t)\}_{p=1}^P$

$$\mu_t(dx) \approx \mu_t^P(dx) = \frac{1}{P} \sum_{j=1}^P \delta_{X_j^P(t)}(dx). \quad (4)$$

Strong convergence of particle systems has been proven for a broad class of $b(\cdot), \sigma(\cdot)$ (Haji-Ali et al., 2021; Bossy and Talay, 1997, 1996; Méléard, 1996). The high dimensionality of the corresponding Fokker-Planck equation, satisfied by the particle system's joint probability density, motivates the use of MC methods, which do not suffer from the curse of dimensionality.

2.1 Running Example: Kuramoto oscillator model

The methodology introduced in this work is tested on the simple, one-dimensional Kuramoto model (Acebrón et al., 2005; Cumin and Unsworth, 2007; Forrester, 2015), which is used to describe synchronization in statistical physics to help model behavior of large sets of coupled oscillators. It is a system of P fully connected, synchronized oscillators. The state of each oscillator is represented by process $X_p^P : [0, T] \times \Omega \rightarrow \mathbb{R}$ that has the following Itô SDE dynamics

$$\begin{cases} dX_p^P(t) = \left(\xi_p + \frac{1}{P} \sum_{q=1}^P \sin(X_p^P(t) - X_q^P(t)) \right) dt + \sigma dW_p(t), \quad t > 0 \\ X_p^P(0) = (x_0)_p \sim \mu_0 \in \mathcal{P}(\mathbb{R}), \end{cases} \quad (5)$$

where $\{\xi_p\}_{p=1}^P$ are iid random variables sampled from a prescribed distribution; diffusion $\sigma \in \mathbb{R}$ is constant; $\{(x_0)_p\}_{p=1}^P$ are iid random variables sampled from $\mu_0 \in \mathcal{P}(\mathbb{R})$; $\{W_p\}_{p=1}^P$ are mutually independent one-dimensional Wiener processes; and $\{\xi_p\}_{p=1}^P, \{(x_0)_p\}_{p=1}^P, \{W_p\}_{p=1}^P$ are mutually independent. The oscillator system (5) reaches mean-field limit as the number

of oscillators tends to infinity, where each particle now behaves according to the following MV-SDE,

$$\begin{cases} dX(t) = \left(\xi + \int_{\mathbb{R}} \sin(X(t) - x) \mu_t(dx) \right) dt + \sigma dW(t), & t > 0 \\ X(0) = x_0 \sim \mu_0 \in \mathcal{P}(\mathbb{R}), \end{cases} \quad (6)$$

where X denotes the mean-field process; ξ is a random variable sampled from some prescribed distribution; and μ_t is the mean-field law of X at time t .

2.2 Problem Setting

Consider the McKean-Vlasov process $X : [0, T] \times \Omega \rightarrow \mathbb{R}^d$ as defined in (1), where $T > 0$ is some finite terminal time. Let $G : \mathbb{R}^d \rightarrow \mathbb{R}$ be a given scalar observable function. Our objective is to build a computationally efficient estimator \mathcal{A} of $\mathbb{E}[G(X(T))]$ that satisfies relative error tolerance $\text{TOL}_r > 0$ in the following sense

$$\mathbb{P} \left[\frac{|\mathcal{A} - \mathbb{E}[G(X(T))]|}{|\mathbb{E}[G(X(T))]|} \geq \text{TOL}_r \right] \leq \nu, \quad (7)$$

for a given confidence level determined by $0 < \nu \ll 1$.

The high-dimensionality of the KBE corresponding to the stochastic particle system (3) makes it challenging to numerically approximate $\mathbb{E}[G(X(T))]$ using standard PDE solvers for a given relative tolerance TOL_r . To overcome this issue, it becomes necessary to employ Monte Carlo (MC) methods, which mitigate the curse of dimensionality. Additionally, the combination of MC with importance sampling (IS), is essential for obtaining feasible estimates of rare events. In Section 3, we introduce the decoupling approach for MV-SDEs, present the associated notation, and introduce the DLMC estimator (Ben Rached et al., 2022a).

3 Double Loop Monte Carlo Estimator

The decoupling approach, as presented in (dos Reis et al., 2023), involves a two-step process. Firstly, an empirical approximation of the McKean-Vlasov law (4) is used to define the decoupled MV-SDE. Secondly, a measure change is applied to this decoupled SDE. This approach separates the estimation of the mean-field law from the necessary change in probability measure for importance sampling (IS). By decoupling these two aspects, we can treat the decoupled MV-SDE as a standard SDE with random coefficients, allowing for a well-formulated change of measure (Newton, 1994; Milstein and Tretyakov, 2004; Hartmann et al., 2017; Hinds and Tretyakov, 2022). In this section, we introduce the general scheme of the decoupling approach, which consists of the following steps, as outlined in (Ben Rached et al., 2022a; dos Reis et al., 2023).

1. The mean field law $\{\mu_t : t \in [0, T]\}$ is approximated using an empirical measure $\{\mu_t^P : t \in [0, T]\}$, derived using (4) with one realization of the P -particle system (3) with particles $\{X_p^P\}_{p=1}^P$.

2. Given $\{\mu_t^P : t \in [0, T]\}$, we define the decoupled MV-SDE. Consider the decoupled McKean-Vlasov process $\bar{X}^P : [0, T] \times \Omega \rightarrow \mathbb{R}^d$ with the following dynamics

$$\begin{cases} d\bar{X}^P(t) = b \left(\bar{X}^P(t), \frac{1}{P} \sum_{j=1}^P \kappa_1(\bar{X}^P(t), X_j^P(t)) \right) dt \\ \quad + \sigma \left(\bar{X}^P(t), \frac{1}{P} \sum_{j=1}^P \kappa_2(\bar{X}^P(t), X_j^P(t)) \right) d\bar{W}(t), \quad t \in [0, T] \\ \bar{X}^P(0) = \bar{x}_0 \sim \mu_0, \quad \bar{x}_0 \in \mathbb{R}^d, \end{cases} \quad (8)$$

where superscript P indicates that the process is conditioned on an empirical law computed with a P -particle system; \bar{W} is a standard d -dimensional Wiener process that is independent of Wiener processes $\{W_p\}_{p=1}^P$ driving the corresponding particle system (3); and $\bar{x}_0 \in \mathbb{R}^d$ is a random initial state sampled from μ_0 and independent from $\{(x_0)_p\}_{p=1}^P$ used in (3). Thus, (8) is a standard SDE for a given realization of the empirical law $\{\mu_t^P : t \in [0, T]\}$.

3. Suppose the particle system (3) is defined on the probability space $(\Omega, \mathcal{F}, \mathbb{P})$. Consider a copy space $(\bar{\Omega}, \bar{\mathcal{F}}, \bar{\mathbb{P}})$ (dos Reis et al., 2023); and we define (8) on the product space $(\Omega, \mathcal{F}, \mathbb{P}) \times (\bar{\Omega}, \bar{\mathcal{F}}, \bar{\mathbb{P}})$. One can look at \mathbb{P} as a probability measure induced by random variables driving the particle system (3) and $\bar{\mathbb{P}}$ as the measure induced by random variables in (8) conditioned on empirical law $\{\mu_t^P : t \in [0, T]\}$.

4. Re-express and approximate the quantity of interest as

$$\begin{aligned} \mathbb{E}[G(X(T))] &\approx \mathbb{E}_{\mathbb{P} \otimes \bar{\mathbb{P}}}[G(\bar{X}^P(T))] \\ &= \mathbb{E}_{\mathbb{P}}[\mathbb{E}_{\bar{\mathbb{P}}}[G(\bar{X}^P(T)) \mid \{\mu_t^P : t \in [0, T]\}]]. \end{aligned} \quad (9)$$

Henceforth, we denote $\mathbb{E}[G(\bar{X}^P(T))] \equiv \mathbb{E}_{\mathbb{P} \otimes \bar{\mathbb{P}}}[G(\bar{X}^P(T))]$ for convenience.

By utilizing the decoupling approach, we represent our quantity of interest as the nested expectation in (9). However, directly approximating the inner expectation $\mathbb{E}_{\bar{\mathbb{P}}}[G(\bar{X}^P(T)) \mid \{\mu_t^P : t \in [0, T]\}]$ by numerically solving the Kolmogorov backward equation for each realization of the empirical law for a relative error tolerance is computationally infeasible. To address this challenge, we employ a nested Monte Carlo average with importance sampling (IS) to estimate the nested expectation (9) in the rare events regime (Ben Rached et al., 2022a). Algorithm 1 outlines the procedure for this estimation. In the algorithm, $\omega_{1:P}^{(i)}$ represents the i^{th} realization of the P sets of random variables (Wiener increments, initial conditions etc.) that drive the dynamics of the interacting P -particle system in (3). Thus, $\{\mu_t^P : t \in [0, T]\}(\omega_{1:P}^{(i)})$ denotes i^{th} realization of the empirical law. Furthermore, let $\tilde{\omega}^{(i)}$ denote the i^{th} realization of the random variables that drive the dynamics of the decoupled MV-SDE (8), conditioned on an empirical law realization.

Algorithm 1: Outline of DLMC algorithm for decoupled MV-SDE

Inputs: P, M_1, M_2 ;

for $i = 1, \dots, M_1$ **do**

 Generate $\{\mu_t^P : t \in [0, T]\}$ $(\omega_{1:P}^{(i)})$ using (3),(4);

for $j = 1, \dots, M_2$ **do**

 Given $\{\mu_t^P : t \in [0, T]\}$ $(\omega_{1:P}^{(i)})$, generate sample path of (8) using $\tilde{\omega}^{(j)}$;

 Compute $G(\bar{X}^P(T))(\omega_{1:P}^{(i)}, \tilde{\omega}^{(j)})$;

end

end

Approximate $\mathbb{E}[G(X(T))]$ by $\frac{1}{M_1} \sum_{i=1}^{M_1} \frac{1}{M_2} \sum_{j=1}^{M_2} G(\bar{X}^P(T))(\omega_{1:P}^{(i)}, \tilde{\omega}^{(j)})$;

4 Importance Sampling for MV-SDEs

Within this section, we present a stochastic optimal control-based importance sampling (IS) measure change for the decoupled MV-SDE (8). Subsequently, we integrate this IS approach into the DLMC Algorithm 1.

4.1 Importance sampling using stochastic optimal control for decoupled MV-SDE

In (Ben Rached et al., 2022a), we applied an optimal measure change to the decoupled MV-SDE that provides a zero-variance DLMC estimator via stochastic optimal control theory. First, we formulate the Hamilton-Jacobi-Bellman (HJB) partial differential equation (PDE) that yields the optimal control for the decoupled MV-SDE.

Proposition 1 (HJB PDE for decoupled MV-SDE (Ben Rached et al., 2022a)). Let decoupled McKean-Vlasov process \bar{X}^P satisfy (8). Consider following Itô SDE for the controlled process $\bar{X}_\zeta^P : [0, T] \times \Omega \rightarrow \mathbb{R}^d$ with control $\zeta(t, x) : [t, T] \times \mathbb{R}^d \rightarrow \mathbb{R}^d$,

$$\left\{ \begin{array}{l} d\bar{X}_\zeta^P(t) = \left(b \left(\bar{X}_\zeta^P(t), \frac{1}{P} \sum_{j=1}^P \kappa_1(\bar{X}_\zeta^P(t), X_j^P(t)) \right) \right. \\ \quad \left. + \sigma \left(\bar{X}_\zeta^P(t), \frac{1}{P} \sum_{j=1}^P \kappa_2(\bar{X}_\zeta^P(t), X_j^P(t)) \right) \zeta(t, \bar{X}_\zeta^P(t)) \right) dt \\ \quad + \sigma \left(\bar{X}_\zeta^P(t), \frac{1}{P} \sum_{j=1}^P \kappa_2(\bar{X}_\zeta^P(t), X_j^P(t)) \right) dW(t), \quad 0 < t < T \\ \bar{X}_\zeta^P(0) = \bar{X}^P(0) = \bar{x}_0 \sim \mu_0. \end{array} \right. \quad (10)$$

Here, the corresponding realization of the empirical law $\{\mu_t^P : t \in [0, T]\}$ is computed beforehand from the particle system (3). The value function $u(t, x)$ that minimizes the second moment (see (Ben Rached et al., 2022a) for derivation) of the MC estimator of

$\mathbb{E} [G(\bar{X}^P(T)) \mid \{\mu_t^P : t \in [0, T]\}]$ with IS is written as

$$u(t, x) = \min_{\zeta \in \mathcal{Z}} \mathbb{E} \left[G^2(\bar{X}_\zeta^P(T)) \exp \left\{ - \int_t^T \|\zeta(s, \bar{X}_\zeta^P(s))\|^2 - 2 \int_t^T \langle \zeta(s, \bar{X}_\zeta^P(s)), dW(s) \rangle \right\} \right. \\ \left. \mid \bar{X}_\zeta^P(t) = x, \{\mu_t^P : t \in [0, T]\} \right]. \quad (11)$$

Assume $u(t, x)$ is bounded, smooth, and non-zero throughout its domain. Define $\gamma(t, x)$ such that $u(t, x) = \exp\{-2\gamma(t, x)\}$. Then $\gamma(t, x)$ satisfies the non-linear HJB equation

$$\begin{cases} \frac{\partial \gamma}{\partial t} + \langle b \left(x, \frac{1}{P} \sum_{j=1}^P \kappa_1(x, X_j^P(t)) \right), \nabla \gamma \rangle + \frac{1}{2} \nabla^2 \gamma : (\sigma \sigma^T) \left(x, \frac{1}{P} \sum_{j=1}^P \kappa_2(x, X_j^P(t)) \right) \\ - \frac{1}{4} \left\| \sigma^T \nabla \gamma \left(x, \frac{1}{P} \sum_{j=1}^P \kappa_2(x, X_j^P(t)) \right) \right\|^2 = 0, \quad (t, x) \in [0, T] \times \mathbb{R}^d \\ \gamma(T, x) = -\log |G(x)|, \quad x \in \mathbb{R}^d, \end{cases} \quad (12)$$

with optimal control

$$\zeta^*(t, x) = -\sigma^T \left(x, \frac{1}{P} \sum_{j=1}^P \kappa_2(x, X_j^P(t)) \right) \nabla \gamma(t, x), \quad (13)$$

which minimizes the second moment of the IS estimator conditioned on $\{\mu_t^P : t \in [0, T]\}$.

Proof. See Appendix B in (Ben Rached et al., 2022a). \square

In proposition 1, $\langle \cdot, \cdot \rangle$ is the Euclidean dot product between two \mathbb{R}^d vectors; $\nabla \cdot$ is the gradient vector of a scalar function; $\nabla^2 \cdot$ is the Hessian matrix of a scalar function; $\cdot : \cdot$ is the Frobenius inner product between two matrix-valued functions; and $\|\cdot\|$ is the Euclidean norm of an \mathbb{R}^d vector. Previous works (Ben Rached et al., 2022a; Awad et al., 2013) have shown that (12) leads to a zero variance estimator of the inner expectation $\mathbb{E} [G(\bar{X}^P(T)) \mid \{\mu_t^P : t \in [0, T]\}]$, provided $G(\cdot)$ does not change sign. Using the transformation $u(t, x) = v^2(t, x)$, one can thus recover the linear KBE corresponding to (8),

$$\begin{cases} \frac{\partial v}{\partial t} + \langle b \left(x, \frac{1}{P} \sum_{j=1}^P \kappa_1(x, X_j^P(t)) \right), \nabla v \rangle \\ + \frac{1}{2} \nabla^2 v : (\sigma \sigma^T) \left(x, \frac{1}{P} \sum_{j=1}^P \kappa_2(x, X_j^P(t)) \right) = 0, \quad (t, x) \in [0, T] \times \mathbb{R}^d \\ v(T, x) = |G(x)|, \quad x \in \mathbb{R}^d, \end{cases} \quad (14)$$

with optimal control

$$\zeta^*(t, x) = \sigma^T \left(x, \frac{1}{P} \sum_{j=1}^P \kappa_2(x, X_j^P(t)) \right) \nabla \log v(t, x). \quad (15)$$

To calculate the control using (14) and (15), a realization of the empirical law is required. However, in order to avoid the computational burden of computing the optimal control for each realization of $\{\mu_t^P : t \in [0, T]\}$ within the DLMC algorithm, we independently obtain an accurate realization of the empirical law offline, by using a sufficiently large number of particles and time steps, as described in Algorithm 2 of our previous work (Ben Rached et al., 2022a). This approach is motivated by the fact that it is sufficient to solve (14) roughly but cheaply to get efficient variance reduction in the IS estimator. We numerically demonstrate this in Section 6.

4.2 DLMC estimator with importance sampling

We briefly outline the DLMC estimator for a given IS control $\zeta : [0, T] \times \mathbb{R}^d \rightarrow \mathbb{R}^d$.

1. Consider uniform discretization $0 = t_0 < t_1 < t_2 < \dots < t_N = T$ of time domain $[0, T]$ with N equal time steps of the particle system (3), i.e., $t_n = n\Delta t$, $n = 0, 1, \dots, N$ and $\Delta t = T/N$. Let us denote by $X_p^{P|N}$ the discretized version of particle X_p^P corresponding to (3) with P particles.
2. Define the discrete law obtained from the time-discretized particle system by $\mu^{P|N}$ as

$$\mu^{P|N}(t_n) = \frac{1}{P} \sum_{j=1}^P \delta_{X_j^{P|N}(t_n)}, \quad \forall n = 0, \dots, N. \quad (16)$$

3. Consider the same time discretization as the particle system (3) for the controlled decoupled MV-SDE (10) with N equal time steps. Let us denote by $\{\bar{X}_\zeta^{P|N}(t_n)\}_{n=1}^N$ the Euler-Maruyama time-discretized version of the controlled, decoupled McKean-Vlasov process $\bar{X}_\zeta^{P|N}$, conditioned on empirical law $\mu^{P|N}$ (16)
4. Thus, we can approximate our quantity of interest with IS as

$$\mathbb{E}[G(X(T))] \approx \mathbb{E}[G(\bar{X}^{P|N}(T))] = \mathbb{E}[G(\bar{X}_\zeta^{P|N}(T)) \mathbb{L}^{P|N}], \quad (17)$$

where the likelihood factor $\mathbb{L}^{P|N}$ (see (Ben Rached et al., 2022a) for derivation) is

$$\mathbb{L}^{P|N} = \prod_{n=0}^{N-1} \exp \left\{ -\frac{1}{2} \Delta t \left\| \zeta(t_n, \bar{X}_\zeta^{P|N}(t_n)) \right\|^2 - \langle \Delta W(t_n), \zeta(t_n, \bar{X}_\zeta^{P|N}(t_n)) \rangle \right\}, \quad (18)$$

and $\{\Delta W(t_n)\}_{n=0}^{N-1} \sim \mathcal{N}(0, \sqrt{\Delta t} \mathbb{I}_d)$ are the Wiener increments used in the time-discretized decoupled MV-SDE (10).

5. Let M_1 be the number of realizations of $\mu^{P|N}$ in the DLMC estimator. Let $\omega_{1:P}^{(i)}$ denote the i^{th} realization of $\omega_{1:P}$. For each realization of $\mu^{P|N}$, let M_2 be the number of sample paths for the decoupled MV-SDE for each $\mu^{P|N}$. Let $\tilde{\omega}^{(j)}$ denote the j^{th} realization of $\tilde{\omega}$. Then, the DLMC estimator \mathcal{A}_{MC} is defined as

$$\mathcal{A}_{\text{MC}} = \frac{1}{M_1} \sum_{i=1}^{M_1} \frac{1}{M_2} \sum_{j=1}^{M_2} G\left(\bar{X}_{\zeta}^{P|N}(T)\right) \mathbb{L}^{P|N}\left(\omega_{1:P}^{(i)}, \tilde{\omega}^{(j)}\right). \quad (19)$$

Remark 1. In (Ben Rached et al., 2022a), we demonstrated that the DLMC estimator with IS in (19), achieves an optimal complexity of $\mathcal{O}(\text{TOL}_r^{-4})$ for prescribed relative error tolerance TOL_r . Moreover, the use of IS ensures that the constant associated with the complexity (19) decreases drastically compared to naive MC, making the computation of rare event probabilities feasible. Furthermore, in our subsequent work (Ben Rached et al., 2022b), we extended the aforementioned DLMC estimator to the multilevel setting. This extension allows for the estimation of expectations of rare event Lipschitz observables up to a relative tolerance of TOL_r , while achieving a reduced complexity of $\mathcal{O}(\text{TOL}_r^{-3})$ for the considered Kuramoto example (5).

The main contribution of this work is represented in Section 5, where we extend this estimator to the multi-index setting to obtain even better complexity.

5 Multi-index Double Loop Monte Carlo

Following (Haji-Ali et al., 2016a), we introduce the multi-index DLMC discretization. As seen in Section 4, two discretization parameters (P, N) are used to generate sample paths of the decoupled MV-SDE. We introduce multi-index $\alpha = (\alpha_1, \alpha_2) \in \mathbb{N}^2$ and $\tau = (\tau_1, \tau_2) \in \mathbb{N}^2$ that define the discretization parameters,

$$\begin{aligned} P_{\alpha_1} &= P_0 \tau_1^{\alpha_1}, \\ N_{\alpha_2} &= N_0 \tau_2^{\alpha_2}. \end{aligned} \quad (20)$$

P_0 and N_0 are the minimum number of particles and time steps used to generate approximate sample paths of the decoupled MV-SDE. Henceforth, we use $\tau_1 = \tau_2 = \tau$ for easier presentation. Let $G = G(X(T))$ and its corresponding discretization $G_{\alpha} = G(\bar{X}^{P_{\alpha_1}|N_{\alpha_2}}(T))$. Following (Haji-Ali et al., 2016a), we define the first order mixed difference for this setting

$$\Delta G_{\alpha} = (G_{(\alpha_1, \alpha_2)} - G_{(\alpha_1-1, \alpha_2)}) - (G_{(\alpha_1, \alpha_2-1)} - G_{(\alpha_1-1, \alpha_2-1)}). \quad (21)$$

The multi-index MC method is based on the following telescoping sum

$$\mathbb{E}[G] = \sum_{\alpha \in \mathbb{N}^2} \mathbb{E}[\Delta G_{\alpha}], \quad (22)$$

with $G_{(-1,0)} = 0$, $G_{(0,-1)} = 0$ and $G_{(-1,-1)} = 0$. Let $\Delta \mathcal{G}_{\alpha}$ be a random variable such that $\mathbb{E}[\Delta \mathcal{G}_{\alpha}] = \mathbb{E}[\Delta G_{\alpha}]$. In the trivial case, $\Delta \mathcal{G}_{\alpha} = \Delta G_{\alpha}$. One can also choose $\Delta \mathcal{G}_{\alpha}$ cleverly

such that $\text{Var}[\Delta\mathcal{G}_\alpha] \ll \text{Var}[\Delta G_\alpha]$. Each of the expectations in (22) is approximated using a DLMC estimator, giving rise to the multi-index DLMC estimator,

$$\mathbb{E}[G] \approx \mathcal{A}_{\text{MIMC}}(\mathcal{I}) = \sum_{\alpha \in \mathcal{I}} \frac{1}{M_{1,\alpha}} \sum_{m_1=1}^{M_{1,\alpha}} \frac{1}{M_{2,\alpha}} \sum_{m_2=1}^{M_{2,\alpha}} \Delta\mathcal{G}_\alpha \left(\omega_{1:P_{\alpha_1}}^{(\alpha, m_1)}, \tilde{\omega}^{(\alpha, m_2)} \right), \quad (23)$$

where $\mathcal{I} \in \mathbb{N}^2$ is an appropriately chosen index-set and $\{M_{1,\alpha}, M_{2,\alpha}\}$ are integer number of samples in the inner and outer loops of the DLMC estimator for each $\alpha \in \mathcal{I}$. Following (Ben Rached et al., 2022b), we construct an antithetic estimator $\Delta\mathcal{G}_\alpha$ defined as

$$\Delta\mathcal{G}_\alpha \left(\omega_{1:P_{\alpha_1}}^{(\alpha, m_1)}, \tilde{\omega}^{(\alpha, m_2)} \right) = \left((G_{(\alpha_1, \alpha_2)} - \mathcal{G}_{(\alpha_1-1, \alpha_2)}) - (G_{(\alpha_1, \alpha_2-1)} - \mathcal{G}_{(\alpha_1-1, \alpha_2-1)}) \right) \left(\omega_{1:P_{\alpha_1}}^{(\alpha, m_1)}, \tilde{\omega}^{(\alpha, m_2)} \right), \quad (24)$$

where $\mathcal{G}_{(\alpha_1-1, \alpha_2)}$ is highly correlated to $G_{(\alpha_1, \alpha_2)}$ and is defined as

$$\mathcal{G}_{(\alpha_1-1, \alpha_2)} \left(\omega_{1:P_{\alpha_1}}^{(\alpha, m_1)}, \tilde{\omega}^{(\alpha, m_2)} \right) = \frac{1}{\tau} \sum_{a=1}^{\tau} G_{(\alpha_1-1, \alpha_2)} \left(\omega_{(a-1)P_{\alpha_1-1}+1:aP_{\alpha_1-1}}^{(\alpha, m_1)}, \tilde{\omega}^{(\alpha, m_2)} \right). \quad (25)$$

In (25), we split the P_{α_1} sets of random variables into τ iid groups of size P_{α_1-1} each and then use each group to independently generate a realization of the empirical law. For each of the τ realizations of the empirical law we generate approximate sample paths of $\bar{X}^{P_{\alpha_1-1}|N_{\alpha_2}}$ using the same $\tilde{\omega}$ as for $G_{(\alpha_1, \alpha_2)}$, before averaging the quantity of interest over the τ groups. From (Ben Rached et al., 2022a), we know that the computational cost of the DLMC estimator with P number of particles, N number of time steps, M_1 number of outer loop samples and M_2 number of inner loop samples in Algorithm 1 is $\mathcal{O}(M_1 N^{\gamma_2} P^{1+\gamma_1} + M_1 M_2 N^{\gamma_2} P^{\gamma_1})$. Here $\gamma_1 > 0$ is the computational complexity rate of estimating the empirical measure in the drift and diffusion coefficients and $\gamma_2 > 0$ is the computational complexity rate of the time discretization scheme. With this, we can express the total computational cost of the multi-index DLMC estimator,

$$\mathcal{W}[\mathcal{A}_{\text{MIMC}}(\mathcal{I})] \lesssim \sum_{\alpha \in \mathcal{I}} M_{1,\alpha} N_{\alpha_2}^{\gamma_2} P_{\alpha_1}^{1+\gamma_1} + M_{1,\alpha} M_{2,\alpha} N_{\alpha_2}^{\gamma_2} P_{\alpha_1}^{\gamma_1}. \quad (26)$$

Notation $a \lesssim b$ means that there exists a constant c independent of b such that $a < cb$. Note that $\Delta\mathcal{G}_\alpha$ requires 4 evaluations of G at different discretization parameters. However, the largest work among them corresponds to the index $\alpha = (\alpha_1, \alpha_2)$. Due to independence of DLMC estimators for each α in (23), the multi-index DLMC estimator variance can be written as

$$\text{Var}[\mathcal{A}_{\text{MIMC}}(\mathcal{I})] = \sum_{\alpha \in \mathcal{I}} \frac{1}{M_{1,\alpha}} \text{Var} \left[\frac{1}{M_{2,\alpha}} \sum_{m_2=1}^{M_{2,\alpha}} \Delta\mathcal{G}_\alpha \left(\omega_{1:P_{\alpha_1}}^{(\alpha, \cdot)}, \tilde{\omega}^{(\alpha, m_2)} \right) \right]. \quad (27)$$

Using the law of total variance,

$$\begin{aligned}\text{Var}[\mathcal{A}_{\text{MIMC}}(\mathcal{I})] &= \sum_{\alpha \in \mathcal{I}} \frac{1}{M_{1,\alpha}} \left(\underbrace{\text{Var}[\mathbb{E}[\Delta \mathcal{G}_\alpha \mid \omega_{1:P_{\alpha_1}}^{(\alpha, \cdot)}]]}_{=V_{1,\alpha}} + \frac{1}{M_{2,\alpha}} \underbrace{\mathbb{E}[\text{Var}[\Delta \mathcal{G}_\alpha \mid \omega_{1:P_{\alpha_1}}^{(\alpha, \cdot)}]]}_{=V_{2,\alpha}} \right) \\ &= \sum_{\alpha \in \mathcal{I}} \left(\frac{V_{1,\alpha}}{M_{1,\alpha}} + \frac{V_{2,\alpha}}{M_{1,\alpha}M_{2,\alpha}} \right).\end{aligned}\quad (28)$$

Here $V_{1,\alpha}$ and $V_{2,\alpha}$ are essentially conditioned on the discretized empirical law $\mu^{P_{\alpha_1}|N_{\alpha_2}}$ which are described by the set of random variables $\omega_{1:P_{\alpha_1}}^{(\alpha, \cdot)}$. Our aim is to build an efficient multi-index DLMC estimator that satisfies (7). We bound the relative error of $\mathcal{A}_{\text{MIMC}}$ as

$$\frac{|\mathbb{E}[G] - \mathcal{A}_{\text{MIMC}}|}{|\mathbb{E}[G]|} \leq \underbrace{\frac{|\mathbb{E}[G] - \mathbb{E}[\mathcal{A}_{\text{MIMC}}]|}{|\mathbb{E}[G]|}}_{=\epsilon_b, \text{ Relative bias}} + \underbrace{\frac{|\mathbb{E}[\mathcal{A}_{\text{MIMC}}] - \mathcal{A}_{\text{MIMC}}|}{|\mathbb{E}[G]|}}_{=\epsilon_s, \text{ Relative statistical error}}. \quad (29)$$

We split the accuracy between relative bias and statistical errors using parameter $\theta \in (0, 1)$ and impose following stricter constraints

$$\epsilon_b \leq (1 - \theta)\text{TOL}_r, \quad (30)$$

$$\mathbb{P}[\epsilon_s \geq \theta\text{TOL}_r] \leq \nu. \quad (31)$$

Throughout this work, θ is assumed to be given and fixed. Detailed analysis of the role of θ can be found in (Collier et al., 2015; Haji-Ali et al., 2016b). Using the asymptotic normality of the multi-index estimator (Haji-Ali et al., 2016a), the statistical error constraint (31) can be approximated by the following constraint on the variance of the estimator

$$\text{Var}[\mathcal{A}_{\text{MIMC}}(\mathcal{I})] = \sum_{\alpha \in \mathcal{I}} \left(\frac{V_{1,\alpha}}{M_{1,\alpha}} + \frac{V_{2,\alpha}}{M_{1,\alpha}M_{2,\alpha}} \right) \leq \left(\frac{\theta\text{TOL}_r\mathbb{E}[G]}{C_\nu} \right)^2, \quad (32)$$

where C_ν is the $(1 - \frac{\nu}{2})$ -quantile of the standard normal distribution. For a given index set \mathcal{I} , we optimize total computational cost (26) with respect to $M_{1,\alpha} \in \mathbb{R}_+$ and $M_{2,\alpha} \in \mathbb{R}_+$ for all $\alpha \in \mathcal{I}$ subject to the statistical error constraint (32).

$$\begin{cases} \min_{\{M_{1,\alpha}, M_{2,\alpha}\}_{\alpha \in \mathcal{I}}} \sum_{\alpha \in \mathcal{I}} M_{1,\alpha} N_{\alpha_2}^{\gamma_2} P_{\alpha_1}^{1+\gamma_1} + M_{1,\alpha} M_{2,\alpha} N_{\alpha_2}^{\gamma_2} P_{\alpha_1}^{\gamma_1} \\ \text{s.t.} \quad \left(\sum_{\alpha \in \mathcal{I}} \frac{V_{1,\alpha}}{M_{1,\alpha}} + \frac{V_{2,\alpha}}{M_{1,\alpha}M_{2,\alpha}} \right) \approx \left(\frac{\theta\text{TOL}_r\mathbb{E}[G]}{C_\nu} \right)^2 \end{cases}. \quad (33)$$

Solution to (33) yields

$$\mathcal{M}_{1,\alpha} = \left(\frac{C_\nu}{\theta\text{TOL}_r\mathbb{E}[G]} \right)^2 \sqrt{\frac{V_{1,\alpha}}{N_{\alpha_2}^{\gamma_2} P_{\alpha_1}^{1+\gamma_1}}} \sum_{\beta \in \mathcal{I}} \left(\sqrt{V_{1,\beta} N_{\beta_2}^{\gamma_2} P_{\beta_1}^{1+\gamma_1}} + \sqrt{V_{2,\beta} N_{\beta_2}^{\gamma_2} P_{\beta_1}^{\gamma_1}} \right),$$

$$\tilde{\mathcal{M}}_{\alpha} = \mathcal{M}_{1,\alpha} \mathcal{M}_{2,\alpha} = \left(\frac{C_{\nu}}{\theta \text{TOL}_{\text{r}} \mathbb{E}[G]} \right)^2 \sqrt{\frac{V_{2,\alpha}}{N_{\alpha_2}^{\gamma_2} P_{\alpha_1}^{\gamma_1}}} \sum_{\beta \in \mathcal{I}} \left(\sqrt{V_{1,\beta} N_{\beta_2}^{\gamma_2} P_{\beta_1}^{1+\gamma_1}} + \sqrt{V_{2,\beta} N_{\beta_2}^{\gamma_2} P_{\beta_1}^{\gamma_1}} \right). \quad (34)$$

In practice, we use natural numbers for $\{\mathcal{M}_{1,\alpha}, \mathcal{M}_{2,\alpha}\}_{\alpha \in \mathcal{I}}$. For this reason, and to guarantee at least one $\mathcal{M}_{1,\alpha}$ and $\mathcal{M}_{2,\alpha}$ for each α , we use following number of samples

$$M_{1,\alpha} = \lceil \mathcal{M}_{1,\alpha} \rceil, \quad M_{2,\alpha} = \left\lceil \frac{\tilde{\mathcal{M}}_{\alpha}}{\lceil \mathcal{M}_{1,\alpha} \rceil} \right\rceil. \quad (35)$$

Using (35) we bound the estimator cost as

$$\begin{aligned} \mathcal{W}[\mathcal{A}_{\text{MIMC}}(\mathcal{I})] &\lesssim \sum_{\alpha \in \mathcal{I}} \left((\mathcal{M}_{1,\alpha} + 1) N_{\alpha_2}^{\gamma_2} P_{\alpha_1}^{1+\gamma_1} + (\mathcal{M}_{1,\alpha} + 1) \left(\frac{\tilde{\mathcal{M}}_{\alpha}}{\lceil \mathcal{M}_{1,\alpha} \rceil} + 1 \right) N_{\alpha_2}^{\gamma_2} P_{\alpha_1}^{\gamma_1} \right) \\ &\leq \underbrace{\sum_{\alpha \in \mathcal{I}} \left(\mathcal{M}_{1,\alpha} N_{\alpha_2}^{\gamma_2} P_{\alpha_1}^{1+\gamma_1} + \tilde{\mathcal{M}}_{\alpha} N_{\alpha_2}^{\gamma_2} P_{\alpha_1}^{\gamma_1} \right)}_{=W_1(\mathcal{I})} + \underbrace{\sum_{\alpha \in \mathcal{I}} (P_{\alpha_1}^{1+\gamma_1} N_{\alpha_2}^{\gamma_2} + P_{\alpha_1}^{\gamma_1} N_{\alpha_2}^{\gamma_2})}_{=W_2(\mathcal{I}), \text{ cost of one sample per multi-index}} \\ &\quad + \underbrace{\sum_{\alpha \in \mathcal{I}} \mathcal{M}_{1,\alpha} N_{\alpha_2}^{\gamma_2} P_{\alpha_1}^{\gamma_1}}_{=W_3(\mathcal{I})} + \underbrace{\sum_{\alpha \in \mathcal{I}} \frac{\tilde{\mathcal{M}}_{\alpha}}{\lceil \mathcal{M}_{1,\alpha} \rceil} N_{\alpha_2}^{\gamma_2} P_{\alpha_1}^{\gamma_1}}_{=W_4(\mathcal{I})}. \end{aligned} \quad (36)$$

Using $P_{\alpha_1} > 0$ and $\gamma_1 > 0$, it is easy to see that,

$$\begin{aligned} W_3(\mathcal{I}) &= \sum_{\alpha \in \mathcal{I}} \mathcal{M}_{1,\alpha} N_{\alpha_2}^{\gamma_2} P_{\alpha_1}^{\gamma_1} \leq \sum_{\alpha \in \mathcal{I}} \mathcal{M}_{1,\alpha} N_{\alpha_2}^{\gamma_2} P_{\alpha_1}^{1+\gamma_1} \leq W_1(\mathcal{I}), \\ W_4(\mathcal{I}) &= \sum_{\alpha \in \mathcal{I}} \frac{\tilde{\mathcal{M}}_{\alpha}}{\lceil \mathcal{M}_{1,\alpha} \rceil} N_{\alpha_2}^{\gamma_2} P_{\alpha_1}^{\gamma_1} \leq \sum_{\alpha \in \mathcal{I}} \frac{\tilde{\mathcal{M}}_{\alpha}}{\max(1, \mathcal{M}_{1,\alpha})} N_{\alpha_2}^{\gamma_2} P_{\alpha_1}^{\gamma_1} \\ &\leq \sum_{\alpha \in \mathcal{I}} \tilde{\mathcal{M}}_{\alpha} N_{\alpha_2}^{\gamma_2} P_{\alpha_1}^{\gamma_1} \leq W_1(\mathcal{I}). \end{aligned}$$

Hence, we can rewrite (36) as follows,

$$\mathcal{W}[\mathcal{A}_{\text{MIMC}}(\mathcal{I})] \lesssim W_1(\mathcal{I}) + W_2(\mathcal{I}). \quad (37)$$

Substituting (34) in (37), we get

$$\begin{aligned} \mathcal{W}[\mathcal{A}_{\text{MIMC}}(\mathcal{I})] &\lesssim \left(\frac{C_{\nu}}{\theta \text{TOL}_{\text{r}} \mathbb{E}[G]} \right)^2 \left(\sum_{\alpha \in \mathcal{I}} \sqrt{V_{1,\alpha} N_{\alpha_2}^{\gamma_2} P_{\alpha_1}^{1+\gamma_1}} + \sqrt{V_{2,\alpha} N_{\alpha_2}^{\gamma_2} P_{\alpha_1}^{\gamma_1}} \right)^2 \\ &\quad + \sum_{\alpha \in \mathcal{I}} (P_{\alpha_1}^{1+\gamma_1} N_{\alpha_2}^{\gamma_2} + P_{\alpha_1}^{\gamma_1} N_{\alpha_2}^{\gamma_2}). \end{aligned} \quad (38)$$

We make the following assumptions in this work.

Assumption 1. For all $\alpha \in \mathcal{I}$, the absolute value of the expected value of $\Delta\mathcal{G}_\alpha$ satisfies

$$|\mathbb{E}[\Delta\mathcal{G}_\alpha]| \leq Q_B \tau^{-\alpha_1 b_1 - \alpha_2 b_2}, \quad (39)$$

for constants $Q_B > 0$ and $b_1, b_2 > 0$.

Assumption 2. For all $\alpha \in \mathcal{I}$, the variance terms in (28) satisfy

$$V_{1,\alpha} = \text{Var} \left[\mathbb{E} \left[\Delta\mathcal{G}_\alpha \mid \omega_{1:P_{\alpha_1}}^{(\alpha, \cdot)} \right] \right] \lesssim \tau^{-\alpha_1 w_1 - \alpha_2 w_2}, \quad (40)$$

$$V_{2,\alpha} = \mathbb{E} \left[\text{Var} \left[\Delta\mathcal{G}_\alpha \mid \omega_{1:P_{\alpha_1}}^{(\alpha, \cdot)} \right] \right] \lesssim \tau^{-\alpha_1 s_1 - \alpha_2 s_2}, \quad (41)$$

for constants $w_i > 0$ and $s_i > 0$ for $i = 1, 2$.

Remark 2. (On Assumptions 1 and 2) Assumption 1 is derived from the bias assumptions made in our previous work (Ben Rached et al., 2022a), which are based on the well-known propagation of chaos in McKean-Vlasov SDEs (where the empirical law converges to the mean-field law) and the standard weak convergence of the Euler-Maruyama time discretization scheme for SDEs. Assumption 2 is motivated by the convergence of variance in the multilevel DLMC estimator introduced in our previous work (Ben Rached et al., 2022b). Currently, there are no formal proofs of these assumptions for particle systems, but we validate them numerically for the Kuramoto model (5) in Section 6.

Under Assumptions 1, 2, total computational cost (38) can be estimated as

$$\mathcal{W}[\mathcal{A}_{\text{MIMC}}(\mathcal{I})] \lesssim \left(\frac{C_\nu}{\theta \text{TOL}_r \mathbb{E}[G]} \right)^2 \left(\underbrace{\sum_{\alpha \in \mathcal{I}} (\exp\{\bar{\mathbf{g}} \cdot \alpha\} + \exp\{\bar{\bar{\mathbf{g}}} \cdot \alpha\})}_{=\tilde{W}_1(\mathcal{I})} \right)^2 + \underbrace{\sum_{\alpha \in \mathcal{I}} \exp\{\lambda \cdot \alpha\}}_{=\tilde{W}_2(\mathcal{I})}, \quad (42)$$

where the vectors $\bar{\mathbf{g}}, \bar{\bar{\mathbf{g}}}, \lambda \in \mathbb{R}^2$ are defined as

$$\bar{\mathbf{g}} = \log(\tau) \left[\frac{1 + \gamma_1 - w_1}{2}, \frac{\gamma_2 - w_2}{2} \right], \quad (43)$$

$$\bar{\bar{\mathbf{g}}} = \log(\tau) \left[\frac{\gamma_1 - s_1}{2}, \frac{\gamma_2 - s_2}{2} \right], \quad (44)$$

$$\lambda = \log(\tau) [1 + \gamma_1, \gamma_2]. \quad (45)$$

It should be noted that $\tilde{W}_2(\mathcal{I})$ represents the total computational cost required to generate one sample for each multi-index $\alpha \in \mathcal{I}$. This is the minimum cost for a DLMC estimator, and it is essential to ensure that it does not dominate the first term in the bound (42). For now, we assume that the first term indeed dominates over the second term, allowing us to focus solely on $\tilde{W}_1(\mathcal{I})$. In the subsequent theorem, we explicitly outline the conditions that guarantee the dominance of the first term.

5.1 Optimal index set

One of the main objectives of this work is to motivate a choice for the set of multi-indices $\mathcal{I} = \mathcal{I}(\text{TOL}_r)$ that minimizes $\mathcal{W}[\mathcal{A}_{\text{MIMC}}(\mathcal{I})]$, subject to the following bias constraint

$$\epsilon_b(\mathcal{I}) = \frac{1}{|\mathbb{E}[G]|} \left| \sum_{\alpha \notin \mathcal{I}} \mathbb{E}[\Delta \mathcal{G}_\alpha] \right| \leq \frac{1}{|\mathbb{E}[G]|} \sum_{\alpha \notin \mathcal{I}} |\mathbb{E}[\Delta \mathcal{G}_\alpha]| \leq (1 - \theta) \text{TOL}_r. \quad (46)$$

Using (39), we rewrite (46) as

$$\tilde{B}(\mathcal{I}) = \sum_{\alpha \notin \mathcal{I}} \exp\{-\boldsymbol{\rho} \cdot \boldsymbol{\alpha}\} \leq \frac{(1 - \theta) \text{TOL}_r \mathbb{E}[G]}{Q_B}, \quad (47)$$

where we define the vector $\boldsymbol{\rho} = \log(\tau) [b_1, b_2] \in \mathbb{R}^2$. $\tilde{B}(\mathcal{I})$ can be seen as an upper bound on the global bias of $\mathcal{A}_{\text{MIMC}}$. To find optimal \mathcal{I} , we solve the following optimization problem

$$\min_{\mathcal{I} \in \mathbb{N}^2} \mathcal{W}[\mathcal{A}_{\text{MIMC}}(\mathcal{I})] \quad \text{such that} \quad \epsilon_b(\mathcal{I}) \leq (1 - \theta) \text{TOL}_r. \quad (48)$$

To simplify the problem we work with the upper bound on the bias (47) and the work (42). We assume that the first term in (42) dominates the second. Subsequently, we solve the following simplified problem to get quasi-optimal set \mathcal{I}

$$\min_{\mathcal{I} \in \mathbb{N}^2} \tilde{W}_1(\mathcal{I}) \quad \text{such that} \quad \tilde{B}(\mathcal{I}) \leq \frac{(1 - \theta) \text{TOL}_r \mathbb{E}[G]}{Q_B}. \quad (49)$$

Note that $\tilde{W}_1(\mathcal{I})$ is defined in (42) and $\tilde{B}(\mathcal{I})$ is defined in (47). For convenience, we refer to the objective \tilde{W}_1 as the "work" and the constraint function \tilde{B} as the "error" in the rest of this section. To solve the optimization problem (49), we closely follow the procedure in (Haji-Ali et al., 2016a). First, we write the total error associated with index set \mathcal{I} from (47) as follows

$$\tilde{B}(\mathcal{I}) = \sum_{\alpha \notin \mathcal{I}} \exp\{-\boldsymbol{\rho} \cdot \boldsymbol{\alpha}\} = \sum_{\alpha \notin \mathcal{I}} \mathcal{E}_\alpha. \quad (50)$$

Here $\mathcal{E}_\alpha = \exp\{-\boldsymbol{\rho} \cdot \boldsymbol{\alpha}\}$ denotes the "error" contribution of multi-index $\boldsymbol{\alpha}$. Next, we write the total "work" using (42) as follows

$$\tilde{W}_1(\mathcal{I}) = \sum_{\alpha \in \mathcal{I}} (\exp\{\bar{\mathbf{g}} \cdot \boldsymbol{\alpha}\} + \exp\{\bar{\bar{\mathbf{g}}} \cdot \boldsymbol{\alpha}\}) = \sum_{\alpha \in \mathcal{I}} \varpi_\alpha. \quad (51)$$

Here $\varpi_\alpha = \exp\{\bar{\mathbf{g}} \cdot \boldsymbol{\alpha}\} + \exp\{\bar{\bar{\mathbf{g}}} \cdot \boldsymbol{\alpha}\}$ denotes the "work" contribution of multi-index $\boldsymbol{\alpha}$. Next, we assign a "profit" indicator to each multi-index and only the most profitable multi-indices are added to the index set \mathcal{I} . Let us define the profit of a multi-index $\boldsymbol{\alpha}$ as follows

$$\mathcal{P}_\alpha = \frac{\mathcal{E}_\alpha}{\varpi_\alpha}. \quad (52)$$

Using (50),(51), we can approximate the profits by

$$\mathcal{P}_\alpha = \frac{\exp\{-\boldsymbol{\rho} \cdot \boldsymbol{\alpha}\}}{\exp\{\bar{\mathbf{g}} \cdot \boldsymbol{\alpha}\} + \exp\{\bar{\bar{\mathbf{g}}} \cdot \boldsymbol{\alpha}\}}. \quad (53)$$

Following (Haji-Ali et al., 2016a), we define optimal index set for given level $v \in \mathbb{R}_+$ as the following level set

$$\mathcal{I}(v) = \{\boldsymbol{\alpha} \in \mathbb{N}^2 : \mathcal{P}_\alpha \geq v\}. \quad (54)$$

Inserting (53) into (54), we get the optimal index set for some $L \in \mathbb{R}_+$ for the multi-index DLMC estimator

$$\mathcal{I}(L) = \left\{ \boldsymbol{\alpha} \in \mathbb{N}^2 : \exp\left\{ \underbrace{(\bar{\mathbf{g}} + \boldsymbol{\rho}) \cdot \boldsymbol{\alpha}}_{=\bar{\boldsymbol{\delta}}} \right\} + \exp\left\{ \underbrace{(\bar{\bar{\mathbf{g}}} + \boldsymbol{\rho}) \cdot \boldsymbol{\alpha}}_{=\bar{\bar{\boldsymbol{\delta}}} \right\} \leq L \right\}. \quad (55)$$

Here $\bar{\boldsymbol{\delta}} = [\bar{\delta}_1, \bar{\delta}_2]$, $\bar{\bar{\boldsymbol{\delta}}} = [\bar{\bar{\delta}}_1, \bar{\bar{\delta}}_2] \in \mathbb{R}_+^2$ are normalised weighting vectors written explicitly as follows

$$\begin{aligned} \bar{\boldsymbol{\delta}} &= \left[\frac{\left(\frac{1+\gamma_1-w_1}{2} + b_1 \right)}{C_{\bar{\boldsymbol{\delta}}}}, \frac{\left(\frac{\gamma_2-w_2}{2} + b_2 \right)}{C_{\bar{\boldsymbol{\delta}}}} \right], \quad C_{\bar{\boldsymbol{\delta}}} = \left(\frac{1+\gamma_1-w_1}{2} + b_1 \right) + \left(\frac{\gamma_2-w_2}{2} + b_2 \right), \\ \bar{\bar{\boldsymbol{\delta}}} &= \left[\frac{\left(\frac{\gamma_1-s_1}{2} + b_1 \right)}{C_{\bar{\bar{\boldsymbol{\delta}}}}}, \frac{\left(\frac{\gamma_2-s_2}{2} + b_2 \right)}{C_{\bar{\bar{\boldsymbol{\delta}}}}} \right], \quad C_{\bar{\bar{\boldsymbol{\delta}}}} = \left(\frac{\gamma_1-s_1}{2} + b_1 \right) + \left(\frac{\gamma_2-s_2}{2} + b_2 \right). \end{aligned} \quad (56)$$

To ensure admissible index sets according to the classical multi-index method (Haji-Ali et al., 2016a), we need that $\bar{\delta}_1, \bar{\delta}_2, \bar{\bar{\delta}}_1, \bar{\bar{\delta}}_2 > 0$. This leads to the following condition on the convergence rates

$$2b_1 \geq \max(w_1 - 1, s_1) - \gamma_1, \quad 2b_2 \geq \max(w_2, s_2) - \gamma_2. \quad (57)$$

For the following theorem, let us introduce the following notation.

$$\begin{aligned} \chi_{11} &= C_{\bar{\boldsymbol{\delta}}} \log(\tau) \max \left(\frac{1+\gamma_1-w_1}{1+\gamma_1-w_1+2b_1}, \frac{\gamma_2-w_2}{\gamma_2-w_2+2b_2} \right), \\ \chi_{12} &= C_{\bar{\boldsymbol{\delta}}} \log(\tau) \max \left(\frac{\gamma_1-s_1}{1+\gamma_1-w_1+2b_1}, \frac{\gamma_2-s_2}{\gamma_2-w_2+2b_2} \right), \\ \chi_{21} &= C_{\bar{\bar{\boldsymbol{\delta}}}(\log)} \tau \max \left(\frac{1+\gamma_1-w_1}{\gamma_1-s_1+2b_1}, \frac{\gamma_2-w_2}{\gamma_2-s_2+2b_2} \right), \\ \chi_{22} &= C_{\bar{\bar{\boldsymbol{\delta}}}(\log)} \log(\tau) \max \left(\frac{\gamma_1-s_1}{\gamma_1-s_1+2b_1}, \frac{\gamma_2-s_2}{\gamma_2-s_2+2b_2} \right), \\ \eta_1 &= C_{\bar{\boldsymbol{\delta}}} \log(\tau) \min \left(\frac{2b_1}{1+\gamma_1-w_1+2b_1}, \frac{2b_2}{\gamma_2-w_2+2b_2} \right), \\ \eta_2 &= C_{\bar{\bar{\boldsymbol{\delta}}}(\log)} \log(\tau) \min \left(\frac{2b_1}{\gamma_1-s_1+2b_1}, \frac{2b_2}{\gamma_2-s_2+2b_2} \right), \end{aligned}$$

$$\begin{aligned}
e_1 &= \begin{cases} 2, & \frac{1+\gamma_1-w_1}{2b_1} = \frac{\gamma_2-w_2}{2b_2} \\ 1, & \text{otherwise} \end{cases}, \quad e_2 = \begin{cases} 2, & \frac{\gamma_1-s_1}{2b_1} = \frac{\gamma_2-s_2}{2b_2} \\ 1, & \text{otherwise} \end{cases}, \\
\aleph_1 &= \begin{cases} 2, & \frac{\gamma_1-s_1}{1+\gamma_1-w_1+2b_1} = \frac{\gamma_2-s_2}{\gamma_2-w_2+2b_2} \\ 1, & \text{otherwise} \end{cases}, \quad \aleph_2 = \begin{cases} 2, & \frac{1+\gamma_1-w_1}{\gamma_1-s_1+2b_1} = \frac{\gamma_2-w_2}{\gamma_2-s_2+2b_2} \\ 1, & \text{otherwise} \end{cases}, \\
d_1 &= \begin{cases} 2, & w_1 = 1 + \gamma_1 \text{ and } w_2 = \gamma_2 \\ 1, & w_1 = 1 + \gamma_1 \text{ or } w_2 = \gamma_2 \\ 0, & \text{otherwise} \end{cases}, \quad d_2 = \begin{cases} 2, & s_1 = \gamma_1 \text{ and } s_2 = \gamma_2 \\ 1, & s_1 = \gamma_1 \text{ or } s_2 = \gamma_2 \\ 0, & \text{otherwise} \end{cases}, \\
\varsigma &= \min \left(\max \left(0, \frac{\chi_{11}}{\eta_1}, \frac{\chi_{12}}{\eta_1} \right), \max \left(0, \frac{\chi_{21}}{\eta_2}, \frac{\chi_{22}}{\eta_2} \right) \right), \\
\varrho &= \begin{cases} \max(d_1, d_2), & \varsigma = 0 \\ (e_1 - 1) \left(1 + \frac{\chi_{11}}{\eta_1} \right), & \varsigma = \frac{\chi_{11}}{\eta_1} \\ (\aleph_1 - 1) + (e_1 - 1) \frac{\chi_{12}}{\eta_1}, & \varsigma = \frac{\chi_{12}}{\eta_1} \\ (\aleph_2 - 1) + (e_2 - 1) \frac{\chi_{21}}{\eta_2}, & \varsigma = \frac{\chi_{21}}{\eta_2} \\ (e_2 - 1) \left(1 + \frac{\chi_{22}}{\eta_2} \right), & \varsigma = \frac{\chi_{22}}{\eta_2} \end{cases}, \\
\Psi &= \min \left(\frac{1 + \gamma_1}{1 + \gamma_1 - w_1 + 2b_1}, \frac{\gamma_2}{\gamma_2 - w_2 + 2b_2}, \frac{1 + \gamma_1}{\gamma_1 - s_1 + 2b_1}, \frac{\gamma_2}{\gamma_2 - s_2 + 2b_2} \right).
\end{aligned}$$

Theorem 1. (*Optimal multi-index DLMC complexity*) Consider the optimal multi-index set given by (55) with optimal vectors $\bar{\delta}$ and $\bar{\delta}$ as defined in (56) and satisfying the condition (57). Under Assumptions 1 and 2, let the optimal $\bar{L} \in \mathbb{R}_+$ satisfy the bias constraint (47) in the following sense

$$\lim_{\text{TOL}_r \downarrow 0} \frac{\tilde{B}(\mathcal{I}(\bar{L}))}{\frac{(1-\theta)\text{TOL}_r \mathbb{E}[G]}{Q_B}} \leq 1. \quad (58)$$

Then, the total computational cost of the multi-index DLMC estimator (23) $\mathcal{W}[\mathcal{A}_{\text{MIMC}}(\mathcal{I}(\bar{L}))]$, subject to constraint (32) satisfies the following

$$\limsup_{\text{TOL}_r \downarrow 0} \frac{\mathcal{W}[\mathcal{A}_{\text{MIMC}}(\mathcal{I}(\bar{L}))]}{\text{TOL}_r^{-2-2\varsigma} (\log \text{TOL}_r^{-1})^{2\varrho}} \leq C_{\text{work}} < \infty, \quad (59)$$

given that the following condition holds

$$\Psi \leq 1 + \varsigma. \quad (60)$$

Proof. See Appendix A. □

Remark 3. (*On isotropic directions*) To show the superiority of the multi-index DLMC estimator over the multilevel DLMC estimator from (Ben Rached et al., 2022b), we look at the case when $\gamma_1 = \gamma_2 = \gamma > 0$, $w_1 = w_2 = s_1 = s_2 = s > 0$ and $b_1 = b_2 = b > 0$. That is, the complexity, bias and variances converge at the same rates in both P and N

directions. One such case is the Kuramoto setting (5) with the smooth, non-rare observable $G(x) = \cos(x)$. From Theorem 1, we have asymptotically as $\text{TOL}_r \rightarrow 0$

$$\mathcal{W}[\mathcal{A}_{\text{MIMC}}] = \begin{cases} \mathcal{O}(\text{TOL}_r^{-2}), & s > 1 + \gamma \\ \mathcal{O}\left(\text{TOL}_r^{-2} (\log \text{TOL}_r^{-1})^2\right), & s = 1 + \gamma \\ \mathcal{O}\left(\text{TOL}_r^{-2 - \frac{1+\gamma-s}{b}}\right), & s < 1 + \gamma \end{cases}. \quad (61)$$

On the other hand, the multilevel DLMC estimator (Ben Rached et al., 2022b) shows the following complexity rates

$$\mathcal{W}[\mathcal{A}_{\text{MLMC}}] = \begin{cases} \mathcal{O}(\text{TOL}_r^{-2}), & s > 1 + 2\gamma \\ \mathcal{O}\left(\text{TOL}_r^{-2} (\log \text{TOL}_r^{-1})^2\right), & s = 1 + 2\gamma \\ \mathcal{O}\left(\text{TOL}_r^{-2 - \frac{1+2\gamma-s}{b}}\right), & s < 1 + 2\gamma \end{cases}. \quad (62)$$

Comparing (61) and (62), one notices that multi-index DLMC has better complexity rates than multilevel DLMC in all regimes of variance convergence rate s with respect to the complexity rate γ . Also notice that the condition (60) for the multi-index DLMC estimator simplifies in this setting to $2b \geq s$. For the multilevel case, we have the more restrictive condition $2b \geq \min(s, 1 + 2\gamma)$ (Ben Rached et al., 2022b). One also deduces that the complexity of the multi-index DLMC estimator is the same as that of a multilevel DLMC estimator with only P as the discretization parameter (as if we generate exact sample paths of the particle system and decoupled MV-SDE). However, the multi-index DLMC requires mixed regularity (in sense of Assumptions 1,2) with respect to P and N while multilevel DLMC only requires ordinary regularity.

Remark 4. (*Kuramoto Model*) We know that $\gamma_1 = 1$ for a naive estimation method of the empirical mean in the drift/diffusion coefficients of the Kuramoto model (5). We also know that $\gamma_2 = 1$ for the Euler-Maruyama scheme with uniform time grid for the type of drift/diffusion coefficients in (5). In this setting with the mollified indicator observable $G(x) = \frac{1}{2}(1 + \tanh(3(x - K)))$, we show numerically in Section 6 that $b_1 = b_2 = 1$, $w_1 = w_2 = s_1 = 2$ and $s_2 = 1.5$. Using Theorem 1 with these values, one can see that the complexity rate of the multilevel DLMC estimator would be $\mathcal{O}\left(\text{TOL}_r^{-2} (\log \text{TOL}_r^{-1})^2\right)$ compared to $\mathcal{O}(\text{TOL}_r^{-3})$ complexity of the multilevel DLMC estimator (Ben Rached et al., 2022b).

5.2 IS scheme for multi-index DLMC estimator

One of the main objectives of this work is to incorporate IS into a multi-index estimator. In this study, we achieve this by computing control ζ once, through the solution of the control PDE (14), as derived in Section 4. This computation is performed using a single realization of the particle system (3) with a large number of particles \bar{P} and time steps \bar{N} . Once this control is obtained, it is applied uniformly across all multi-indices $\alpha \in \mathcal{I}$ in the multi-index estimator (23). Using IS, we rewrite the quantity of interest as follows

$$\mathbb{E}[G] \approx \sum_{\alpha \in \mathcal{I}} \mathbb{E}[\Delta G_{\alpha}] = \sum_{\alpha \in \mathcal{I}} \mathbb{E}[\Delta G_{\alpha}^{\text{IS}}], \quad (63)$$

where the new IS sample of the mixed difference is defined as,

$$\begin{aligned} \Delta G_{\alpha}^{\text{IS}} = & \left(G_{(\alpha_1, \alpha_2)}^{\zeta} \mathbb{L}_{(\alpha_1, \alpha_2)} - G_{(\alpha_1-1, \alpha_2)}^{\zeta} \mathbb{L}_{(\alpha_1-1, \alpha_2)} \right) \\ & - \left(G_{(\alpha_1, \alpha_2-1)}^{\zeta} \mathbb{L}_{(\alpha_1, \alpha_2-1)} - G_{(\alpha_1-1, \alpha_2-1)}^{\zeta} \mathbb{L}_{(\alpha_1-1, \alpha_2-1)} \right). \end{aligned} \quad (64)$$

Here, $G_{(\alpha_1, \alpha_2)}^{\zeta} = G\left(\bar{X}_{\zeta}^{P_{\alpha_1}|N_{\alpha_2}}(T)\right)$ and the discretized likelihood factor at multi-index α is given by

$$\mathbb{L}_{\alpha} = \prod_{n=0}^{N_{\alpha_2}-1} \exp \left\{ -\frac{1}{2} \frac{T}{N_{\alpha_2}} \left\| \zeta(t_n, \alpha, \bar{X}_{\zeta}^{P_{\alpha_1}|N_{\alpha_2}}(t_n, \alpha)) \right\|^2 - \langle \Delta W(t_n, \alpha), \zeta(t_n, \alpha, \bar{X}_{\zeta}^{P_{\alpha_1}|N_{\alpha_2}}(t_n, \alpha)) \rangle \right\}. \quad (65)$$

$\bar{X}_{\zeta}^{P_{\alpha_1}|N_{\alpha_2}}$ is the discretized, controlled, decoupled MV-SDE process (10), $\{\Delta W(t_n, \alpha)\}_{n=1}^{N_{\alpha_2}} \sim \mathcal{N}\left(0, \sqrt{\frac{T}{N_{\alpha_2}}} \mathbb{I}_d\right)$ are the Wiener increments driving the process $\bar{X}_{\zeta}^{P_{\alpha_1}|N_{\alpha_2}}$ and $\{t_n, \alpha\}_{n=1}^{N_{\alpha_2}}$ are the corresponding time discretization grid points. The proposed multi-index DLMC estimator with IS is written as

$$\mathbb{E}[G] \approx \mathcal{A}_{\text{MIMC}}^{\text{IS}}(\mathcal{I}) = \sum_{\alpha \in \mathcal{I}} \frac{1}{M_{1,\alpha}} \sum_{i=1}^{M_{1,\alpha}} \frac{1}{M_{2,\alpha}} \sum_{j=1}^{M_{2,\alpha}} \Delta \mathcal{G}_{\alpha}^{\text{IS}}(\omega_{1:P_{\alpha_1}}^{(\alpha,i)}, \tilde{\omega}^{(\alpha,j)}). \quad (66)$$

Here, the antithetic IS sampler is defined as

$$\begin{aligned} \Delta \mathcal{G}_{\alpha}^{\text{IS}}\left(\omega_{1:P_{\alpha_1}}^{(\alpha,m_1)}, \tilde{\omega}^{(\alpha,m_2)}\right) = & \left(\left(G_{(\alpha_1, \alpha_2)}^{\text{IS}} - \mathcal{G}_{(\alpha_1-1, \alpha_2)}^{\text{IS}} \right) \right. \\ & \left. - \left(G_{(\alpha_1, \alpha_2-1)}^{\text{IS}} - \mathcal{G}_{(\alpha_1-1, \alpha_2-1)}^{\text{IS}} \right) \right) \left(\omega_{1:P_{\alpha_1}}^{(\alpha,m_1)}, \tilde{\omega}^{(\alpha,m_2)} \right), \end{aligned} \quad (67)$$

where $G_{(\alpha_1, \alpha_2)}^{\text{IS}} = G_{(\alpha_1, \alpha_2)}^{\zeta} \mathbb{L}_{(\alpha_1, \alpha_2)}$ and

$$\mathcal{G}_{(\alpha_1-1, \alpha_2)}^{\text{IS}}\left(\omega_{1:P_{\alpha_1}}^{(\alpha,m_1)}, \tilde{\omega}^{(\alpha,m_2)}\right) = \frac{1}{\tau} \sum_{a=1}^{\tau} G_{(\alpha_1-1, \alpha_2)}^{\text{IS}}\left(\omega_{(a-1)P_{\alpha_1}-1+1:aP_{\alpha_1}-1}^{(\alpha,m_1)}, \tilde{\omega}^{(\alpha,m_2)}\right). \quad (68)$$

Remark 5. In this work, the computation of the IS control ζ is performed offline and independent of the multi-index α . In our previous study (Ben Rached et al., 2022a), we demonstrate that ζ leads to a zero-variance estimator for $\mathbb{E}[G(\bar{X}^P(T)) \mid \{\mu_t^P : t \in [0, T]\}]$. However, it should be emphasized that this does not imply optimal minimization of $\text{Var}[\Delta G_{\alpha}]$. The task of obtaining an α -dependent control using stochastic optimal control, which minimizes $\text{Var}[\Delta G_{\alpha}]$, is left for future research.

Algorithm 2 outlines the implementation of above IS scheme to estimate $\mathbb{E}[\Delta G_{\alpha}]$ for each $\alpha \in \mathcal{I}$, that is required for the multi-index DLMC estimator (66).

Algorithm 2: IS scheme to estimate $\mathbb{E}[\Delta G_\alpha]$

Inputs: $\alpha, M_1, M_2, \zeta(\cdot, \cdot)$;

for $m_1 = 1, \dots, M_1$ **do**

 Generate realization of random variables $\omega_{1:P_{\alpha_1}}^{(\alpha, m_1)}$;

 Using $\omega_{1:P_{\alpha_1}}^{(\alpha, m_1)}$, generate realization of empirical law μ at all required discretizations as per (67) by generating sample paths of particle system (3);

for $m_2 = 1, \dots, M_2$ **do**

 Generate realization of random variables $\tilde{\omega}^{(\alpha, m_2)}$;

 Using $\tilde{\omega}^{(\alpha, m_2)}$, generate sample path of (10) at all required discretizations as per (67) with control ζ ;

 Compute $\Delta \mathcal{G}_\alpha^{\text{IS}}(\omega_{1:P_{\alpha_1}}^{(\alpha, m_1)}, \tilde{\omega}^{(\alpha, m_2)})$ using (67);

end

end

Approximate $\mathbb{E}[\Delta G_\alpha]$ by $\frac{1}{M_1} \sum_{m_1=1}^{M_1} \frac{1}{M_2} \sum_{m_2=1}^{M_2} \Delta \mathcal{G}_\alpha^{\text{IS}}(\omega_{1:P_{\alpha_1}}^{(\alpha, m_1)}, \tilde{\omega}^{(\alpha, m_2)})$;

5.3 Adaptive multi-index DLMC algorithm with importance sampling

The purpose of this section is to develop an adaptive multi-index DLMC algorithm that sequentially selects the index set \mathcal{I} and determines the optimal number of samples $\{M_{1,\alpha}, M_{2,\alpha}\}_{\alpha \in \mathcal{I}}$ to satisfy the error constraints specified in (30) and (31). To accomplish this, the adaptive algorithm relies on cost-effective yet reliable estimations of the relative bias and variances $\{V_{1,\alpha}, V_{2,\alpha}\}_{\alpha \in \mathcal{I}}$. This algorithm is a modified version of the MIMC algorithm presented in (Haji-Ali et al., 2016a).

5.3.1 Estimating bias of index set \mathcal{I}

The optimal index set (55) is defined using the parameter or threshold, L . Given that $\mathcal{I}(L) \subset \mathcal{I}(L+1)$, we use the following heuristic estimate (Haji-Ali et al., 2016a) for the absolute bias corresponding to index-set $\mathcal{I}(L)$

$$|\mathbb{E}[G - \mathcal{A}_{\text{MIMC}}^{\text{IS}}(\mathcal{I}(L))]| \approx \sum_{\alpha \in \partial \mathcal{I}(L)} |\mathbb{E}[\Delta G_\alpha^{\text{IS}}]|, \quad (69)$$

where $\partial \mathcal{I}(L)$ is the outer boundary of the index set $\mathcal{I}(L)$ and is defined as follows

$$\partial \mathcal{I}(L) = \{\alpha \in \mathcal{I}(L) : \alpha + (1, 0) \notin \mathcal{I}(L) \text{ or } \alpha + (0, 1) \notin \mathcal{I}(L)\}. \quad (70)$$

Since $\partial \mathcal{I}(L) \subset \mathcal{I}(L)$, we use already computed nested averages using optimal $\{M_{1,\alpha}, M_{2,\alpha}\}_{\alpha \in \partial \mathcal{I}(L)}$ in (66) to estimate each of the expectations in (69).

5.3.2 Estimating $\{V_{1,\alpha}, V_{2,\alpha}\}$

One needs cheap and robust empirical estimates of $\{V_{1,\alpha}, V_{2,\alpha}\}$ for all $\alpha \in \mathcal{I}(L)$ to compute the optimal number of samples required to satisfy the variance constraint (32) of the estimator using (35). For this, Algorithm 3 with appropriately chosen \tilde{M}_1, \tilde{M}_2 is used.

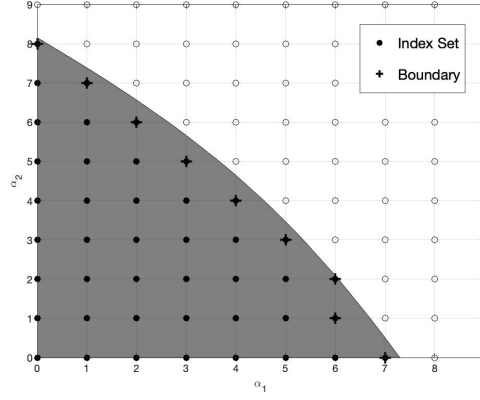


Figure 1: For some index set \mathcal{I} , we visualise the outer boundary of the index set $\partial\mathcal{I}$ as defined in (70).

Algorithm 3: Estimating $\{V_{1,\alpha}, V_{2,\alpha}\}$ for adaptive multi-index DLMC

Inputs: $\alpha, M_1, M_2, \zeta(\cdot, \cdot)$;

for $m_1 = 1, \dots, M_1$ **do**

 Generate realization of random variables $\omega_{1:P_{\alpha_1}}^{(\alpha, m_1)}$;

 Using $\omega_{1:P_{\alpha_1}}^{(\alpha, m_1)}$, generate realization of empirical law μ at all required discretizations as per (67) by generating sample paths of particle system (3);

for $m_2 = 1, \dots, M_2$ **do**

 Generate realization of random variables $\tilde{\omega}^{(\alpha, m_2)}$;

 Using $\tilde{\omega}^{(\alpha, m_2)}$, generate sample path of (10) at all required discretizations as per (67) with control ζ ;

 Compute $\Delta\mathcal{G}_{\alpha}^{\text{IS}}(\omega_{1:P_{\alpha_1}}^{(\alpha, m_1)}, \tilde{\omega}^{(\alpha, m_2)})$ using (67);

end

 Approximate $\mathbb{E} [\Delta\mathcal{G}_{\alpha}^{\text{IS}} \mid \omega_{1:P_{\alpha_1}}^{(\alpha, m_1)}]$ by $\frac{1}{M_2} \sum_{m_2=1}^{M_2} \Delta\mathcal{G}_{\alpha}^{\text{IS}}(\omega_{1:P_{\alpha_1}}^{(\alpha, m_1)}, \tilde{\omega}^{(\alpha, m_2)})$;

 Approximate $\text{Var} [\Delta\mathcal{G}_{\alpha}^{\text{IS}} \mid \omega_{1:P_{\alpha_1}}^{(\alpha, m_1)}]$ by sample variance of

$$\left\{ \Delta\mathcal{G}_{\alpha}^{\text{IS}}(\omega_{1:P_{\alpha_1}}^{(\alpha, m_1)}, \tilde{\omega}^{(\alpha, m_2)}) \right\}_{m_2=1}^{M_2};$$

end

Approximate $V_{1,\alpha}$ by sample variance of $\left\{ \mathbb{E} [\Delta\mathcal{G}_{\alpha}^{\text{IS}} \mid \omega_{1:P_{\alpha_1}}^{(\alpha, m_1)}] \right\}_{m_1=1}^{M_1}$;

Approximate $V_{2,\alpha}$ by $\frac{1}{M_1} \sum_{m_1=1}^{M_1} \text{Var} [\Delta\mathcal{G}_{\alpha}^{\text{IS}} \mid \omega_{1:P_{\alpha_1}}^{(\alpha, m_1)}]$.

Estimating $\{V_{1,\alpha}, V_{2,\alpha}\}$ for all $\alpha \in \mathcal{I}(L)$ using Algorithm 3 can become computationally burdensome when $\mathcal{I}(L)$ is even moderately large. To alleviate this computational overload, we leverage Assumption 2 and employ an extrapolation approach to estimate $\{V_{1,\alpha}, V_{2,\alpha}\}$ for deeper multi-indices. Specifically, we utilize Algorithm 3 solely to estimate $\{V_{1,\alpha}, V_{2,\alpha}\}$ for the small full tensor index set $\{0, 1, 2\} \times \{0, 1, 2\}$. Then, we employ the extrapolation Algorithm 4, making use of Assumption 2, to estimate $\{V_{1,\alpha}, V_{2,\alpha}\}$ for the remaining multi-indices. To further alleviate computational burden, we only estimate $\{V_{1,\alpha}, V_{2,\alpha}\}$ for the newly added multi-indices in each iteration, i.e. for $\alpha \in \mathcal{I}(L+1) \setminus \mathcal{I}(L)$. As $\mathcal{I}(L) \subset \mathcal{I}(L+1)$ by construction, we can reuse the estimates of $\{V_{1,\alpha}, V_{2,\alpha}\}$ for multi-indices from previous iterations.

Algorithm 4: Sample variance extrapolation for adaptive MIDLMC

Inputs: $\mathcal{I}, \{\bar{M}_1, \bar{M}_2\}, \tau, (w_1, w_2), (s_1, s_2);$
Estimate $\{V_{1,\alpha}, V_{2,\alpha}\}$ for $\alpha \in \{0, 1, 2\} \times \{0, 1, 2\}$ using Algorithm 3 with $\{\bar{M}_1, \bar{M}_2\};$
for $\alpha \in \mathcal{I}$ **do**
 if $\alpha_1 = 0, 1$ **then**
 $V_{1,\alpha} = \max\left(\frac{V_{1,\alpha-(0,1)}}{\tau^{w_2}}, \frac{V_{1,\alpha-(0,2)}}{\tau^{2w_2}}\right); V_{2,\alpha} = \max\left(\frac{V_{2,\alpha-(0,1)}}{\tau^{s_2}}, \frac{V_{2,\alpha-(0,2)}}{\tau^{2s_2}}\right);$
 else if $\alpha_2 = 0, 1$ **then**
 $V_{1,\alpha} = \max\left(\frac{V_{1,\alpha-(1,0)}}{\tau^{w_1}}, \frac{V_{1,\alpha-(2,0)}}{\tau^{2w_1}}\right); V_{2,\alpha} = \max\left(\frac{V_{2,\alpha-(1,0)}}{\tau^{s_1}}, \frac{V_{2,\alpha-(2,0)}}{\tau^{2s_1}}\right);$
 else
 $V_{1,\alpha} = \max\left(\frac{V_{1,\alpha-(0,1)}}{\tau^{w_2}}, \frac{V_{1,\alpha-(1,0)}}{\tau^{w_1}}\right); V_{2,\alpha} = \max\left(\frac{V_{2,\alpha-(0,1)}}{\tau^{s_2}}, \frac{V_{2,\alpha-(1,0)}}{\tau^{s_1}}\right);$
 end
end

5.3.3 Relative error control

To meet the relative error constraints (30) and (32) for a given relative error tolerance TOL_r , the adaptive algorithm requires a heuristic estimate of the quantity of interest $\mathbb{E}[G]$ itself. In our algorithm, we update this estimate at each iteration L . For $L = 0$, we utilize Algorithm 2 with appropriately selected \bar{M}_1 and \bar{M}_2 to obtain an initial estimate \bar{G} for $\mathbb{E}[G_{(0,0)}]$. In subsequent iterations, we employ the multi-index estimator (66) with optimal values of $\{M_{1,\alpha}, M_{2,\alpha}\}_{\alpha \in \mathcal{I}(L)}$ to update \bar{G} as well as the absolute error tolerances. Combining all the aforementioned components, we present the adaptive multi-index DLMC algorithm 5 for evaluating rare event observables associated with MV-SDEs. The IS control ζ in Algorithm 5 is computed offline by generating one realization of the empirical law $\mu^{\bar{P}|\bar{N}}$ with some large \bar{P}, \bar{N} and then numerically solving control PDE (14) given $\mu^{\bar{P}|\bar{N}}$.

Remark 6. In Algorithm 5, it is evident that in order to determine the optimal index set $\mathcal{I}(L)$ using equation (55), it is necessary to estimate the rates $\{b_1, b_2\}, \{w_1, w_2\}, \{s_1, s_2\}, \{\gamma_1, \gamma_2\}$ associated with Assumptions 1 and 2. To obtain these estimates, reliable pilot runs are required. It is important to note that such pilot runs are not necessary for the adaptive DLMC algorithm (Ben Rached et al., 2022a) or the multi-level DLMC algorithm (Ben Rached et al., 2022b) described in our previous works.

Algorithm 5: Adaptive multi-index DLMC with IS

User Provided Input: $P_0, N_0, \text{TOL}_r, \zeta(\cdot, \cdot), \nu, \theta, \{\bar{M}_1, \bar{M}_2\}, \{\tilde{M}_1, \tilde{M}_2\}, \{\beta_1, \beta_2\}$;
Input from Pilots: $\{b_1, b_2\}, \{w_1, w_2\}, \{s_1, s_2\}, \{\gamma_1, \gamma_2\}$;
Estimate $\bar{G} = \mathbb{E}[\Delta G_{(0,0)}]$ using **Algorithm 2** with $\bar{M}_1, \bar{M}_2, \zeta(\cdot, \cdot)$;
Estimate and store $\{V_{1,\alpha}, V_{2,\alpha}\}$ for $\alpha \in [0, 1, 2] \times [0, 1, 2]$ using **Algorithm 3** with $\bar{M}_1, \bar{M}_2, \zeta(\cdot, \cdot)$;
Set $L = 1$;
while $\epsilon_b(\mathcal{I}(L)) > (1 - \theta)\text{TOL}_r$ **do**
 Generate index set $\mathcal{I}(L)$ from (55);
 Estimate and store $\{V_{1,\alpha}, V_{2,\alpha}\}_{\alpha \in \mathcal{I}(L)}$ using **Algorithm 4**;
 Compute optimal sample sizes $\{M_{1,\alpha}, M_{2,\alpha}\}_{\alpha \in \mathcal{I}(L)}$ using (35);
 Reevaluate $\bar{G} = \sum_{\alpha \in \mathcal{I}(L)} \mathbb{E}[\Delta G_{\alpha}^{\text{IS}}]$ as per (66) with $\{M_{1,\alpha}, M_{2,\alpha}\}, \zeta(\cdot, \cdot)$ using **Algorithm 2** for each α ;
 $\epsilon_b(\mathcal{I}(L)) \approx \frac{1}{|\bar{G}|} \sum_{\alpha \in \partial \mathcal{I}(L)} |\mathbb{E}[\Delta G_{\alpha}^{\text{IS}}]|$;
 $L \leftarrow L + 1$;
end
 $\mathcal{A}_{\text{MIMC}}^{\text{IS}} = \bar{G}$.

6 Numerical Results

This section provides numerical evidence for the assumptions and complexity rates derived in Section 5. We also numerically validate the efficiency of the IS scheme introduced in Section 5.2 for the multi-index DLMC estimator. The results outlined below focus on the Kuramoto model (see Section 2.1) with the following parameter settings: $\sigma = 0.4$, $T = 1$, $x_0 \sim \mathcal{N}(0, 0.2)$, and $\xi \sim \mathcal{U}(-0.2, 0.2)$. We fix parameters $\tau = 2$, $\theta = 0.5$, and $\nu = 0.05$. We set

$$P_{\alpha_1} = 5 \times 2^{\alpha_1}, \quad N_{\alpha_2} = 4 \times 2^{\alpha_2}. \quad (71)$$

We implement the proposed multi-index DLMC method for the following rare-event observable, also known as the "mollified" indicator function

$$G(x) = \frac{1}{2} (1 + \tanh(3(x - K))), \quad (72)$$

where $K \in \mathbb{R}$ is a threshold parameter that determines how rare the event is. In the following results, we use $K = 3.5$, which corresponds to $\mathbb{E}[G] \approx 2.04 \times 10^{-5}$. We test two methods: multilevel DLMC as outlined in (Ben Rached et al., 2022b) and multi-index DLMC (66) with the index set defined in (55). For both methods, we use an IS control ζ obtained from (15) described in Section 4.2 by simulating a particle system (3) offline with $\bar{P} = 1000$ particles and $\bar{N} = 100$ time steps. The solution to the offline problem (14) was obtained using finite differences with linear interpolation over the entire domain. Our initial analysis focused on verifying the reduction in variance for the DLMC estimators of the mixed difference $\mathbb{E}[\Delta G_{\alpha}]$. Figure 2 illustrates the squared coefficient of variation for the estimator of $\mathbb{E}[\Delta G_{\alpha}]$ with and without importance sampling, plotted as a function of

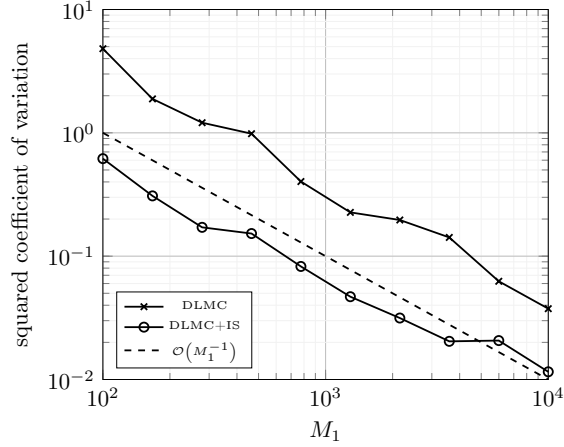


Figure 2: Kuramoto example, numerical variance reduction: Squared coefficient of variation of DLMC estimator for $\mathbb{E}[\Delta G_{(2,2)}]$ with and without IS with respect to the number of sample paths in the outer loop M_1 for fixed $M_2 = 100$.

M_1 with a fixed M_2 . The results in Figure 2 demonstrate a significantly reduced squared coefficient of variation (around one order of magnitude) for the fixed $\alpha = (2, 2)$. It is worth noting that both variances decrease with $\mathcal{O}(M_1^{-1})$, and IS decreases the associated constant. Subsequently, we examine the impact of our IS scheme on all multi-indices $\alpha \in \mathbb{N}^2$. To evaluate this, we analyze the following ratio:

$$\mathcal{R}(\mathcal{A}) = \frac{\text{Var}[\mathcal{A}_{\text{IS}}]}{\text{Var}[\mathcal{A}_{\text{MC}}]}. \quad (73)$$

Here, \mathcal{A}_{IS} and \mathcal{A}_{MC} denote the DLMC estimators of some quantity of interest ($\mathbb{E}[G_\alpha]$ or $\mathbb{E}[\Delta G_\alpha]$) with and without IS respectively. On the left (Figure 3a), we present a contour plot illustrating the values of the ratio \mathcal{R} for the DLMC estimator of $\mathbb{E}[G_\alpha]$ across different $\alpha \in \mathbb{N}^2$, representing the quantity of interest approximated with discretization parameters defined by α . One sees in Figure 3a that there is significant and uniform variance reduction for the DLMC estimator of $\mathbb{E}[G_\alpha]$ for all α . This is expected since our IS control ζ has been constructed to minimize the variance of the corresponding estimator (Ben Rached et al., 2022a). On the right (Figure 3b), we depict the same plot for the DLMC estimator of $\mathbb{E}[\Delta G_\alpha]$ across different $\alpha \in \mathbb{N}^2$. Even though there is still good variance reduction achieved by the same IS control ζ , we observe that this effect diminishes as we delve into deeper multi-indices for the mixed differences estimator.

Figures 4 and 5 provide confirmation of Assumptions 1 and 2 while also numerically determining the convergence rates $\{b_1, b_2\}, \{w_1, w_2\}, \{s_1, s_2\}$ for the above-considered Kuramoto example. In Figure 4a, the convergence of $|\mathbb{E}[\Delta G_\alpha]|$ is plotted to obtain the rates $b_1 = 1$ and $b_2 = 1$. Additionally, Figures 4b and 4c showcase the convergence of $V_{1,\alpha}$ and $V_{2,\alpha}$ for the mixed differences, respectively, yielding the rates $w_1 = 2$, $w_2 = 2$, $s_1 = 2$, and $s_2 = 1.5$. These convergence rates are compared to those of the level differences, $\mathbb{E}[\Delta G_\ell] = \mathbb{E}[G_\ell - G_{\ell-1}]$, utilized in the multilevel DLMC estimator with IS (Ben Rached et al., 2022b). Notably, the mixed differences of the multi-index DLMC estimator exhibit

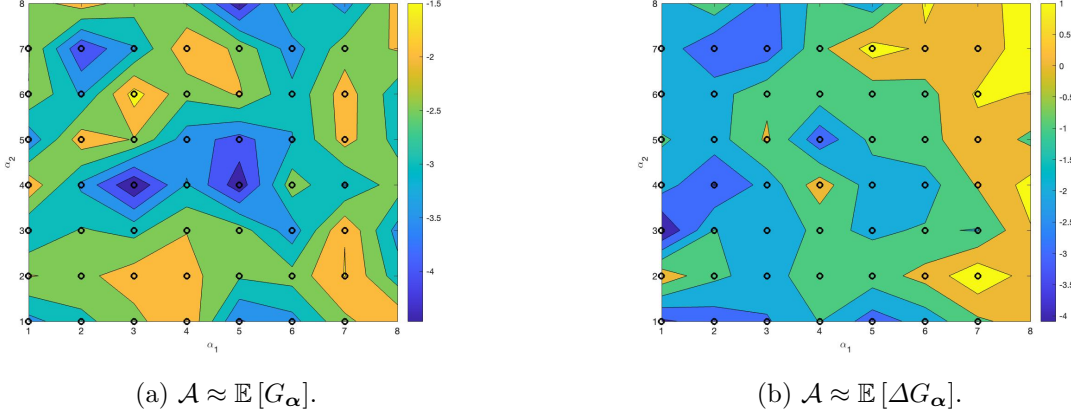


Figure 3: Kuramoto example, numerical variance reduction: Contour plots (log-scale) of $\mathcal{R}(\mathcal{A})$ for a set of $\alpha \in \mathbb{N}^2$ for the estimator of two different quantities, $\mathbb{E}[G_{\alpha}]$ (left) and $\mathbb{E}[\Delta G_{\alpha}]$ (right).

higher convergence rates compared to the level differences of the multi-level estimator. For computational cost analysis, we know that $\gamma_1 = 1$ since the cost of naively estimating the empirical mean in the drift and diffusion coefficients of the particle system (3) is $\mathcal{O}(P)$ with respect to the number of particles. Additionally, we know $\gamma_2 = 1$ as the computational complexity of the uniform Euler-Maruyama time discretization scheme is $\mathcal{O}(N)$.

Figure 5 additionally shows that Assumptions 1 and 2 are indeed satisfied for sufficiently fine discretizations. Using the rates obtained in Figures 4 and 5 we can explicitly write down the optimal index set for the considered Kuramoto example

$$\mathcal{I}(L) = \left\{ \alpha \in \mathbb{N}^2 : \exp\left(\frac{2}{3}\alpha_1 + \frac{1}{3}\alpha_2\right) + \exp\left(\frac{2}{5}\alpha_1 + \frac{3}{5}\alpha_2\right) \leq L \right\}. \quad (74)$$

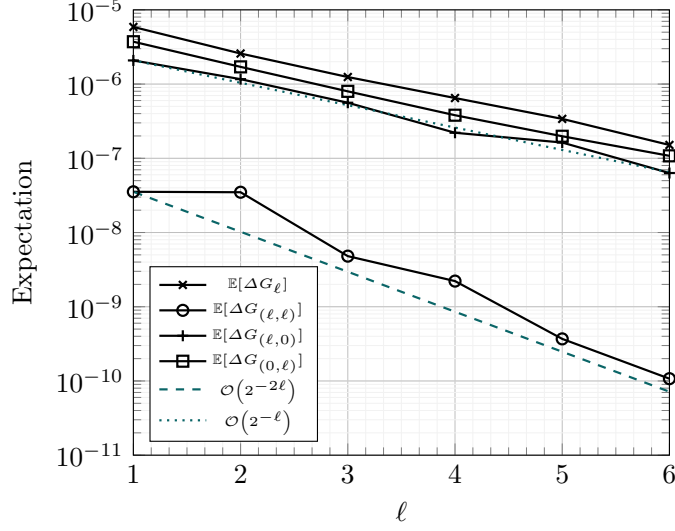
We plug the above rates in Theorem 1 and we expect the work complexity of multi-index DLMC with the index set (74) to be $\mathcal{O}\left(\text{TOL}_r^{-2} (\log \text{TOL}_r^{-1})^2\right)$. Also, the condition (60) for multi-index DLMC is satisfied. For the corresponding multilevel convergence rates obtained in Figure 4, we expect work complexity of $\mathcal{O}(\text{TOL}_r^{-3})$ for the multilevel DLMC estimator (Ben Rached et al., 2022b).

We plot the index-set (74) for different values of L in Figure 6b. We compare this to the index-set obtained with actual numerical profit computed as follows

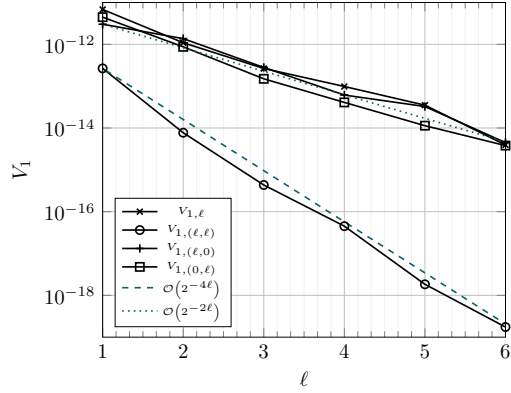
$$\mathcal{I}(v) = \left\{ \alpha \in \mathbb{N}^2 : \mathcal{P}_{\alpha} = \frac{\mathcal{E}_{\alpha}}{\varpi_{\alpha}} \approx \frac{|\mathbb{E}[\Delta G_{\alpha}]|}{\sqrt{V_{1,\alpha} P_{\alpha_1}^2 N_{\alpha_2}} + \sqrt{V_{2,\alpha} P_{\alpha_1} N_{\alpha_2}}} \geq v \right\}. \quad (75)$$

We use DLMC estimates of $|\mathbb{E}[\Delta G_{\alpha}]|$, $V_{1,\alpha}$, $V_{2,\alpha}$ computed in Figure 5 to approximate the numerical profits in (75) to produce Figure 6a. We see that (74) is a reasonable approximation to (75), for sufficiently fine discretizations.

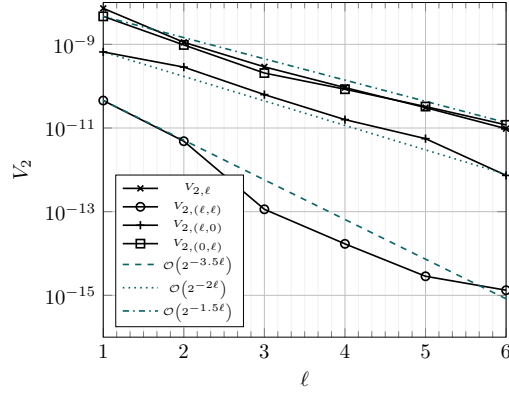
Figures 7-9 depict the results of running the adaptive multi-index DLMC Algorithm 5 with IS and comparing them with the results obtained from the adaptive multilevel algorithm in (Ben Rached et al., 2022b). We employ the parameter values $\{\bar{M}_1, \bar{M}_2\} =$



(a) Verifying (39) from Assumption 1 using Algorithm 2 with $M_1 = 10^3$ and $M_2 = 10^3$.

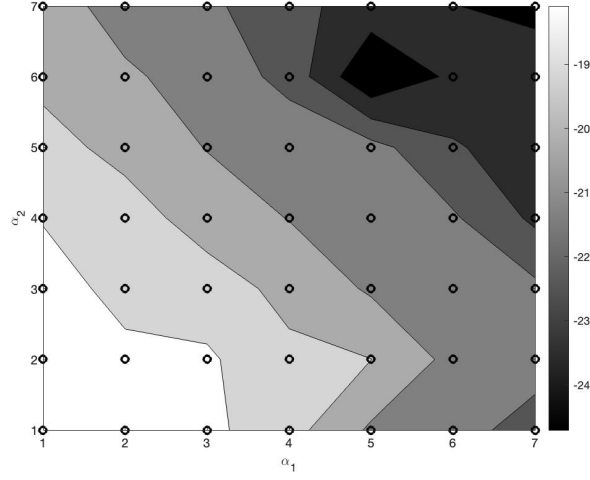


(b) Verifying (40) from Assumption 2 using Algorithm 3 with $M_1 = 10^2$ and $M_2 = 10^4$.

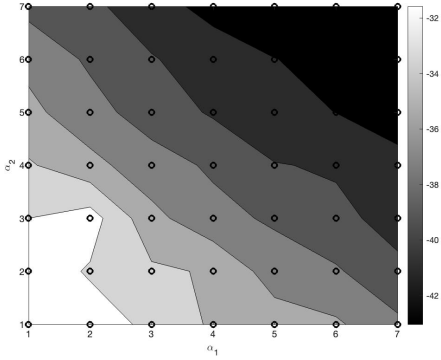


(c) Verifying (40) from Assumption 2 using Algorithm 3 with $M_1 = 10^2$ and $M_2 = 10^4$.

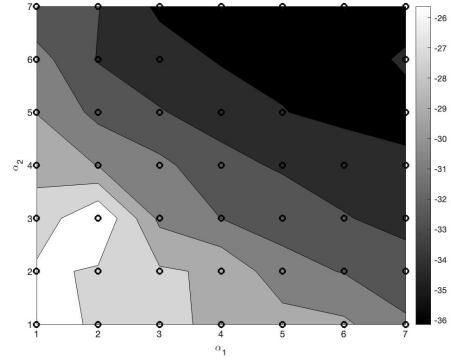
Figure 4: Kuramoto example, numerical rate verification: Sample means and variances of mixed differences used in multi-index DLMC estimator with IS (66).



(a) Contour plots of sample mean $|\mathbb{E}[\Delta G_{\alpha}]|$ of the mixed differences used in the multi-index DLMC estimator (66) obtained using Algorithm 2 with $M_1 = 10^3$ and $M_2 = 10^2$.

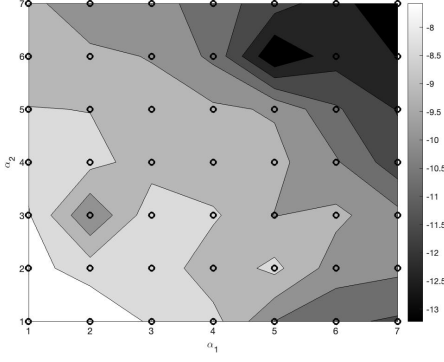


(b) Contour plots of sample $V_{1,\alpha}$ of the mixed differences used in the multi-index DLMC estimator (66) obtained using Algorithm 3 with $M_1 = 10^2$ and $M_2 = 10^3$.

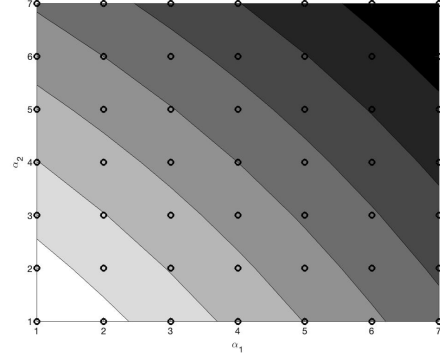


(c) Contour plots of sample $V_{2,\alpha}$ of the mixed differences used in the multi-index DLMC estimator (66) obtained using Algorithm 2 with $M_1 = 10^2$ and $M_2 = 10^3$.

Figure 5: Kuramoto example, numerical rate verification: Contour plots of sample mean and variances used in multi-index DLMC estimator (66). All plots numerically verify Assumptions 1,2 asymptotically.



(a) Contour plot of numerical profits of index set (75).



(b) Contour plot of optimal index sets defined as in (55).

Figure 6: Kuramoto example, optimal index sets: Comparing actual and approximate profits of multi-indices used in the multi-index DLMC estimator (66)

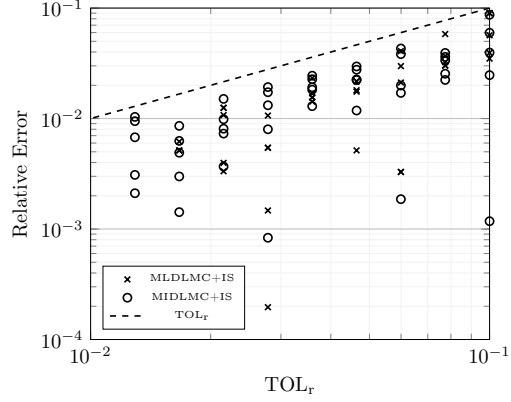
$\{10^3, 10^2\}$ and $\{\tilde{M}_1, \tilde{M}_2\} = \{25, 100\}$. Algorithm 5 and the corresponding multilevel Algorithm, are independently executed five times each, and the combined results are plotted. Figure 7a displays the exact computational relative error achieved by our proposed multi-index DLMC estimator with IS for various prescribed relative tolerances TOL_r , as estimated using a reference multi-index DLMC approximation with $\text{TOL}_r = 1\%$. Each marker represents a separate run of the corresponding adaptive algorithm. Figure 7a confirms that both the multi-index and multilevel estimators satisfy the prescribed TOL_r , in the sense of (7). Figure 7b illustrates the maximum level of discretization required for both the number of particles and time steps in order for both the multilevel and multi-index estimators to satisfy the relative bias constraint (30). In the above Kuramoto model setting, we observe that the maximum number of particles is approximately the same for both the multilevel and multi-index estimators.

In Figure 8, we present a plot of the various error estimates computed during the execution of Algorithm 5. Figure 8a displays the estimated relative bias at the final iteration of Algorithm 5, which is calculated using (69). Furthermore, Figure 8b showcases the estimated relative statistical error of our estimator $\mathcal{A}_{\text{MIMC}}(\mathcal{I})$. As per the algorithm's design, both relative errors should remain below $\frac{\text{TOL}_r}{2}$ for Algorithm 5 to terminate. Moreover, Figure 8b verifies that the number of samples chosen in (35), for our estimator $\mathcal{A}_{\text{MIMC}}(\mathcal{I})$, is indeed optimal.

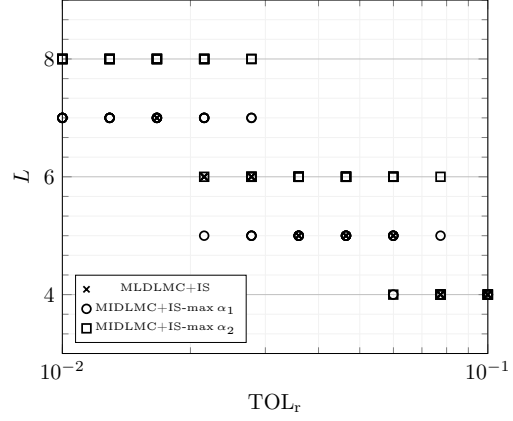
In Figure 9a, we present the average computational runtime of Algorithm 5 for various relative error tolerances. Additionally, Figure 9b displays the average computational cost of both estimators for different values of TOL_r , computed using (26). That is,

$$\text{Computational Cost}[\mathcal{A}_{\text{MIMC}}(\mathcal{I})] \approx \sum_{\alpha \in \mathcal{I}(L)} (M_{1,\alpha} N_{\alpha_2} P_{\alpha_1}^2 + M_{1,\alpha} M_{2,\alpha} N_{\alpha_2} P_{\alpha_1}). \quad (76)$$

Figure 9 also highlights that the adaptive multilevel algorithm failed to produce estimates of the quantity of interest up to $\text{TOL}_r = 1\%$, while the multi-index algorithm

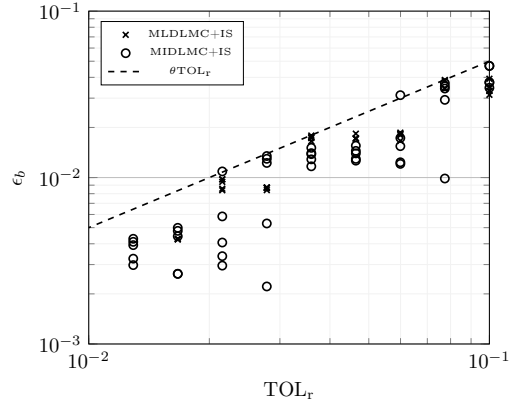


(a) Exact computational relative error for multilevel and multi-index DLMC estimators with IS.

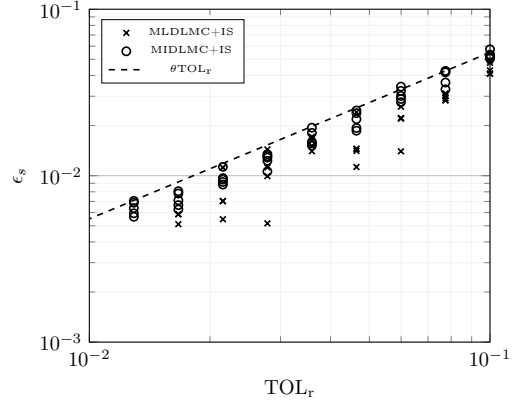


(b) Maximum discretization level of the number of time steps and the number of particles for both multi-index and multilevel DLMC estimators for different tolerances.

Figure 7: Kuramoto example, adaptive DLMC Algorithm with IS: Comparing multilevel and multi-index estimators for $K = 3.5$.

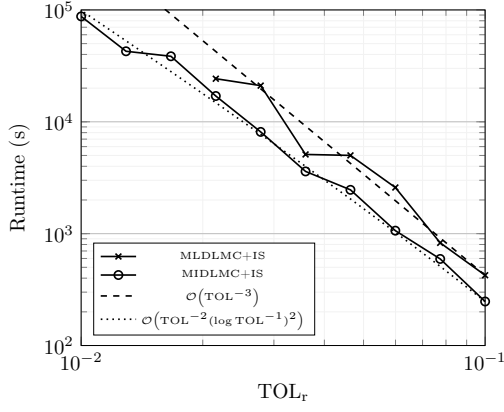


(a) Estimated computational relative bias for multilevel and multi-index estimator with IS.

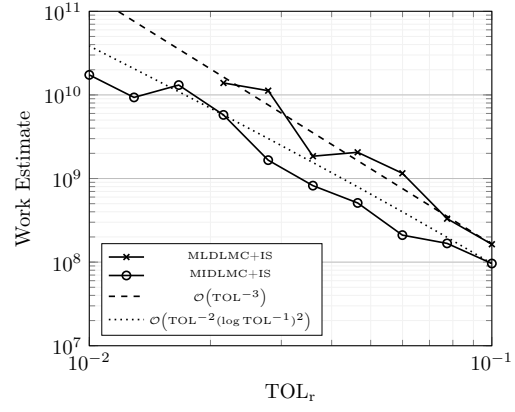


(b) Estimated computational relative statistical error for multilevel and multi-index DLMC estimators with IS.

Figure 8: Kuramoto example, adaptive DLMC Algorithm with IS: Comparing multilevel and multi-index estimators for $K = 3.5$.



(a) Average computational runtime for different values of TOL_r .



(b) Average computational cost estimate for different values of TOL_r .

Figure 9: Kuramoto example, adaptive DLMC Algorithm with IS: Comparing multilevel and multi-index estimators for $K = 3.5$.

achieved it within a fixed computational budget. Furthermore, Figures 9a and 9b provide further evidence supporting the superiority of the proposed multi-index DLMC estimator over the multilevel DLMC estimator. The multi-index estimator demonstrates a complexity reduction of approximately one order (with logarithmic terms) compared to the multilevel estimator in the Kuramoto setting considered. Moreover, Figure 9 also indicates that the complexity rates derived in this work are reasonably accurate.

7 Conclusion

This paper provides theoretical and numerical evidence, under certain verifiable assumptions, of the superiority of our multi-index DLMC estimator over the multilevel DLMC estimator (Ben Rached et al., 2022b) when approximating rare event quantities of interest in the MV-SDE context. These quantities are expressed as expectations of sufficiently smooth observables of solutions to stochastic particle systems in the mean field limit. We utilize the IS scheme introduced in our previous work (Ben Rached et al., 2022a) uniformly for all mixed difference estimators within the proposed multi-index DLMC estimator. Numerical results confirm significant variance reduction and computational gains. For the example considered, the proposed multi-index DLMC estimator achieves a complexity of $\mathcal{O}(\text{TOL}_r^{-2}(\log \text{TOL}_r^{-1})^2)$, which is one order less than that of the multilevel DLMC estimator, where TOL_r is the prescribed relative error tolerance. Integrating the IS scheme into the multilevel MC estimator significantly reduces the constant associated with its complexity compared to the multi-index MC estimator for smooth, non-rare observables introduced in (Haji-Ali and Tempone, 2018).

Future research directions involve extending the IS scheme to higher-dimensional problems by employing model reduction techniques or utilizing stochastic gradient-based learning methods to solve the associated higher-dimensional stochastic optimal control problem. Further optimization of the multi-index DLMC algorithm could involve finding optimal pa-

rameters $\boldsymbol{\tau}$ and θ (Haji-Ali et al., 2016b) or integrating a continuation-type multi-index algorithm (Collier et al., 2015). Furthermore, extending the present analysis to numerically handle non-smooth rare event observables, such as indicator functions for computing rare event probabilities, is an area for exploration.

A Proof of Theorem 1

We begin by writing the optimal index set (55) explicitly for given level $v \in \mathbb{R}_+$

$$\mathcal{I}(v) = \left\{ \boldsymbol{\alpha} \in \mathbb{N}^2 : \frac{\exp\{-\boldsymbol{\rho} \cdot \boldsymbol{\alpha}\}}{\exp\{\bar{\mathbf{g}} \cdot \boldsymbol{\alpha}\} + \exp\{\bar{\bar{\mathbf{g}}} \cdot \boldsymbol{\alpha}\}} \geq v \right\}. \quad (77)$$

We make use of the following optimality result to prove Theorem 1.

Lemma 1. (*Optimal Index Sets*) The set $\mathcal{I}(v) = \left\{ \boldsymbol{\alpha} \in \mathbb{N}^2 : \frac{\exp\{-\boldsymbol{\rho} \cdot \boldsymbol{\alpha}\}}{\exp\{\bar{\mathbf{g}} \cdot \boldsymbol{\alpha}\} + \exp\{\bar{\bar{\mathbf{g}}} \cdot \boldsymbol{\alpha}\}} \geq v \right\}$ is optimal in the sense that any other set $\bar{\mathcal{I}}$ such that $\tilde{B}(\mathcal{I}(v)) = \tilde{B}(\bar{\mathcal{I}})$ will be a set with larger work, i.e. $\tilde{W}_1(\mathcal{I}(v)) \leq \tilde{W}_1(\bar{\mathcal{I}})$.

Proof. We have that for any $\boldsymbol{\alpha} \in \mathcal{I}(v)$ and $\hat{\boldsymbol{\alpha}} \notin \mathcal{I}(v)$

$$\frac{\exp\{-\boldsymbol{\rho} \cdot \boldsymbol{\alpha}\}}{\exp\{\bar{\mathbf{g}} \cdot \boldsymbol{\alpha}\} + \exp\{\bar{\bar{\mathbf{g}}} \cdot \boldsymbol{\alpha}\}} \geq v, \quad (78)$$

$$\frac{\exp\{-\boldsymbol{\rho} \cdot \hat{\boldsymbol{\alpha}}\}}{\exp\{\bar{\mathbf{g}} \cdot \hat{\boldsymbol{\alpha}}\} + \exp\{\bar{\bar{\mathbf{g}}} \cdot \hat{\boldsymbol{\alpha}}\}} < v. \quad (79)$$

Let us divide \mathbb{N}^2 into the following disjoint sets:

$$\begin{aligned} \mathcal{J}_1 &= \mathcal{I}(v) \cap \bar{\mathcal{I}}^C, & \mathcal{J}_2 &= \mathcal{I}(v) \cap \bar{\mathcal{I}}, \\ \mathcal{J}_3 &= \mathcal{I}(v)^C \cap \bar{\mathcal{I}}, & \mathcal{J}_4 &= \mathcal{I}(v)^C \cap \bar{\mathcal{I}}^C, \end{aligned}$$

where $\mathcal{I}(v)^C$ is the complement of the set $\mathcal{I}(v)$. By construction of $\bar{\mathcal{I}}$, we have that

$$\begin{aligned} \tilde{B}(\mathcal{I}(v)) &= \tilde{B}(\bar{\mathcal{I}}) \\ \sum_{\boldsymbol{\alpha} \in \mathcal{J}_3 \cup \mathcal{J}_4} \exp\{-\boldsymbol{\rho} \cdot \boldsymbol{\alpha}\} &= \sum_{\boldsymbol{\alpha} \in \mathcal{J}_1 \cup \mathcal{J}_4} \exp\{-\boldsymbol{\rho} \cdot \boldsymbol{\alpha}\} \\ \sum_{\boldsymbol{\alpha} \in \mathcal{J}_3} \exp\{-\boldsymbol{\rho} \cdot \boldsymbol{\alpha}\} &= \sum_{\boldsymbol{\alpha} \in \mathcal{J}_1} \exp\{-\boldsymbol{\rho} \cdot \boldsymbol{\alpha}\}. \end{aligned} \quad (80)$$

Note that \mathcal{J}_1 and \mathcal{J}_3 cannot be empty, for sets which satisfy $\tilde{B}(\mathcal{I}(v)) = \tilde{B}(\bar{\mathcal{I}})$, unless $\mathcal{I}(v) = \bar{\mathcal{I}}$. Consider the difference between the work of the two sets,

$$\tilde{W}_1(\mathcal{I}(v)) - \tilde{W}_1(\bar{\mathcal{I}}) = \sum_{\boldsymbol{\alpha} \in \mathcal{J}_1 \cup \mathcal{J}_2} \exp\{\bar{\mathbf{g}} \cdot \boldsymbol{\alpha}\} + \exp\{\bar{\bar{\mathbf{g}}} \cdot \boldsymbol{\alpha}\} - \sum_{\boldsymbol{\alpha} \in \mathcal{J}_2 \cup \mathcal{J}_3} \exp\{\bar{\mathbf{g}} \cdot \boldsymbol{\alpha}\} + \exp\{\bar{\bar{\mathbf{g}}} \cdot \boldsymbol{\alpha}\} \quad (81)$$

$$= \sum_{\boldsymbol{\alpha} \in \mathcal{J}_1} \exp\{\bar{\mathbf{g}} \cdot \boldsymbol{\alpha}\} + \exp\{\bar{\bar{\mathbf{g}}} \cdot \boldsymbol{\alpha}\} - \sum_{\boldsymbol{\alpha} \in \mathcal{J}_3} \exp\{\bar{\mathbf{g}} \cdot \boldsymbol{\alpha}\} + \exp\{\bar{\bar{\mathbf{g}}} \cdot \boldsymbol{\alpha}\}. \quad (82)$$

We know from (78) and (79) that

$$\forall \alpha \in \mathcal{J}_1, \quad \exp\{\bar{\mathbf{g}} \cdot \alpha\} + \exp\{\bar{\bar{\mathbf{g}}} \cdot \alpha\} \leq \frac{1}{v} \exp\{-\rho \cdot \alpha\} \quad \text{and}, \quad (83)$$

$$\forall \alpha \in \mathcal{J}_3, \quad -\exp\{\bar{\mathbf{g}} \cdot \alpha\} - \exp\{\bar{\bar{\mathbf{g}}} \cdot \alpha\} < -\frac{1}{v} \exp\{-\rho \cdot \alpha\}. \quad (84)$$

Inserting (83),(84) into (82), we get

$$\begin{aligned} \tilde{W}_1(\mathcal{I}(v)) - \tilde{W}_1(\bar{\mathcal{I}}) &\leq \frac{1}{v} \underbrace{\left(\sum_{\alpha \in \mathcal{J}_1} \exp\{-\rho \cdot \alpha\} - \sum_{\alpha \in \mathcal{J}_3} \exp\{-\rho \cdot \alpha\} \right)}_{=0 \text{ from (80)}} \\ &\Rightarrow \tilde{W}_1(\mathcal{I}(v)) \leq \tilde{W}_1(\bar{\mathcal{I}}). \end{aligned}$$

□

Since the index set $\mathcal{I}(v)$ is optimal in the sense of Lemma 1, we bound $\tilde{W}_1(\mathcal{I}(v))$ by the optimal work done by an index set that can be analysed following the classical multi-index setting (Haji-Ali et al., 2016a). From the definition of the optimal index set (55), there are two obvious candidates for such index sets.

$$\mathcal{I}_{\bar{\delta}}(\bar{L}) = \{\alpha \in \mathbb{N}^2 : \bar{\delta} \cdot \alpha \leq \bar{L}\}, \quad (85)$$

$$\mathcal{I}_{\bar{\bar{\delta}}}(\bar{L}) = \{\alpha \in \mathbb{N}^2 : \bar{\bar{\delta}} \cdot \alpha \leq \bar{L}\}. \quad (86)$$

We now analyse the optimal work of the two index sets separately.

Set 1: $\mathcal{I}_{\bar{\delta}}$

Following (Haji-Ali et al., 2016a), we know there exists an $\bar{L}_1 \in \mathbb{R}_+$ such that the following bias constraint is satisfied.

$$\lim_{\text{TOL}_r \downarrow 0} \frac{\tilde{B}(\mathcal{I}_{\bar{\delta}}(\bar{L}_1))}{\frac{(1-\theta)\text{TOL}_r \mathbb{E}[G]}{Q_B}} \leq 1. \quad (87)$$

For \bar{L} that satisfies (87), let us estimate the work of the corresponding index set.

$$\begin{aligned} \tilde{W}_1(\mathcal{I}_{\bar{\delta}}(\bar{L}_1)) &= \sum_{\{\alpha \in \mathbb{N}^2 : \bar{\delta} \cdot \alpha \leq \bar{L}_1\}} (\exp\{\bar{\mathbf{g}} \cdot \alpha\} + \exp\{\bar{\bar{\mathbf{g}}} \cdot \alpha\}) \\ &= \underbrace{\sum_{\{\alpha \in \mathbb{N}^2 : \bar{\delta} \cdot \alpha \leq \bar{L}_1\}} \exp\{\bar{\mathbf{g}} \cdot \alpha\}}_{=\tilde{W}_{11}} + \underbrace{\sum_{\{\alpha \in \mathbb{N}^2 : \bar{\delta} \cdot \alpha \leq \bar{L}_1\}} \exp\{\bar{\bar{\mathbf{g}}} \cdot \alpha\}}_{=\tilde{W}_{12}}. \end{aligned} \quad (88)$$

From (Haji-Ali et al., 2016a), we know that asymptotically as $\text{TOL}_r \rightarrow 0$,

$$\tilde{W}_{11} \lesssim \begin{cases} (\log \text{TOL}_r^{-1})^{d_1}, & \chi_{11} \leq 0 \\ \text{TOL}_r^{-\frac{\chi_{11}}{\eta_1}} (\log \text{TOL}_r^{-1})^{j_{11}}, & \chi_{11} > 0 \end{cases}, \quad (89)$$

and

$$\tilde{W}_{12} \lesssim \begin{cases} (\log \text{TOL}_r^{-1})^{d_2}, & \chi_{12} \leq 0 \\ \text{TOL}_r^{-\frac{\chi_{12}}{\eta_1}} (\log \text{TOL}_r^{-1})^{j_{12}}, & \chi_{12} > 0 \end{cases}, \quad (90)$$

where we have the following additional notation.

$$\begin{aligned} j_{11} &= (e_1 - 1) \left(1 + \frac{\chi_{11}}{\eta_1} \right), \\ j_{12} &= (\aleph_1 - 1) + (e_1 - 1) \frac{\chi_{11}}{\eta_1}. \end{aligned}$$

Set 2: $\mathcal{I}_{\bar{\delta}}$

Following (Haji-Ali et al., 2016a), we know there exists an $\bar{L}_2 \in \mathbb{R}_+$ such that the bias constraint (87) is satisfied. The work of the corresponding index set is written as

$$\begin{aligned} \tilde{W}_1(\mathcal{I}_{\bar{\delta}}(\bar{L}_2)) &= \sum_{\{\alpha \in \mathbb{N}^2: \bar{\delta} \cdot \alpha \leq \bar{L}_2\}} (\exp\{\bar{\mathbf{g}} \cdot \alpha\} + \exp\{\bar{\bar{\mathbf{g}}} \cdot \alpha\}) \\ &= \underbrace{\sum_{\{\alpha \in \mathbb{N}^2: \bar{\delta} \cdot \alpha \leq \bar{L}_2\}} \exp\{\bar{\mathbf{g}} \cdot \alpha\}}_{=\tilde{W}_{21}} + \underbrace{\sum_{\{\alpha \in \mathbb{N}^2: \bar{\bar{\delta}} \cdot \alpha \leq \bar{L}_2\}} \exp\{\bar{\bar{\mathbf{g}}} \cdot \alpha\}}_{=\tilde{W}_{22}}. \end{aligned} \quad (91)$$

From (Haji-Ali et al., 2016a), we know that asymptotically as $\text{TOL}_r \rightarrow 0$,

$$\tilde{W}_{21} \lesssim \begin{cases} (\log \text{TOL}_r^{-1})^{d_1}, & \chi_{21} \leq 0 \\ \text{TOL}_r^{-\frac{\chi_{21}}{\eta_2}} (\log \text{TOL}_r^{-1})^{j_{21}}, & \chi_{21} > 0 \end{cases}, \quad (92)$$

and

$$\tilde{W}_{22} \lesssim \begin{cases} (\log \text{TOL}_r^{-1})^{d_2}, & \chi_{22} \leq 0 \\ \text{TOL}_r^{-\frac{\chi_{22}}{\eta_2}} (\log \text{TOL}_r^{-1})^{j_{22}}, & \chi_{22} > 0 \end{cases}, \quad (93)$$

where we have the following additional constants.

$$\begin{aligned} j_{21} &= (\aleph_2 - 1) + (e_2 - 1) \frac{\chi_{21}}{\eta_2}, \\ j_{22} &= (e_2 - 1) \left(1 + \frac{\chi_{22}}{\eta_2} \right). \end{aligned}$$

From Lemma 1, we can bound the optimal work of the index set (55) as follows

$$\tilde{W}_1(\mathcal{I}(v_1)) \leq \min \left(\tilde{W}_1(\mathcal{I}_{\bar{\delta}}(\bar{L}_1)), \tilde{W}_1(\mathcal{I}_{\bar{\bar{\delta}}}(\bar{L}_2)) \right). \quad (94)$$

Inserting (89), (90) into (88) and (92), (93) into (91) and combining all into (94), we obtain

$$\tilde{W}_1(\mathcal{I}(v_1)) \lesssim \text{TOL}_r^{-\varsigma} (\log \text{TOL}_r^{-1})^\varrho. \quad (95)$$

Let us also analyse $\tilde{W}_2(\mathcal{I}(v_1))$ since we need to ensure that this work does not dominate the first term in (42). Following the same analysis of the work as for \tilde{W}_1 , we have

$$\begin{aligned} \tilde{W}_2(\mathcal{I}(v_1)) &= \sum_{\{\alpha \in \mathbb{N}^2: \exp\{\bar{\delta} \cdot \alpha\} + \exp\{\bar{\bar{\delta}} \cdot \alpha\} \leq L\}} \exp\{\lambda \cdot \alpha\} \\ &\leq \min \left(\sum_{\{\alpha \in \mathbb{N}^2: \bar{\delta} \cdot \alpha \leq \bar{L}\}} \exp\{\lambda \cdot \alpha\}, \sum_{\{\alpha \in \mathbb{N}^2: \bar{\bar{\delta}} \cdot \alpha \leq \bar{L}\}} \exp\{\lambda \cdot \alpha\} \right). \end{aligned} \quad (96)$$

From (Haji-Ali et al., 2016a) we know that

$$\sum_{\{\alpha \in \mathbb{N}^2: \bar{\delta} \cdot \alpha \leq \bar{L}\}} \exp\{\lambda \cdot \alpha\} \lesssim \text{TOL}_r^{-\frac{\Gamma_1}{\eta_1}} (\log \text{TOL}_r^{-1})^{m_1}, \quad (97)$$

$$\sum_{\{\alpha \in \mathbb{N}^2: \bar{\bar{\delta}} \cdot \alpha \leq \bar{L}\}} \exp\{\lambda \cdot \alpha\} \lesssim \text{TOL}_r^{-\frac{\Gamma_2}{\eta_2}} (\log \text{TOL}_r^{-1})^{m_2}. \quad (98)$$

where we define the following constants,

$$\begin{aligned} \Gamma_1 &= 2C_{\bar{\delta}} \log \tau \min \left(\frac{1 + \gamma_1}{1 + \gamma_1 - w_1 + 2b_1}, \frac{\gamma_2}{\gamma_2 - w_2 + 2b_2} \right), \\ \Gamma_2 &= 2C_{\bar{\bar{\delta}}} \log \tau \min \left(\frac{1 + \gamma_1}{\gamma_1 - s_1 + 2b_1}, \frac{\gamma_2}{\gamma_2 - s_2 + 2b_2} \right), \\ g_1 &= \begin{cases} 2, & \frac{1 + \gamma_1}{1 + \gamma_1 - w_1 + 2b_1} = \frac{\gamma_2}{\gamma_2 - w_2 + 2b_2} \\ 1, & \text{otherwise} \end{cases}, \\ g_2 &= \begin{cases} 2, & \frac{1 + \gamma_1}{\gamma_1 - s_1 + 2b_1} = \frac{\gamma_2}{\gamma_2 - s_2 + 2b_2} \\ 1, & \text{otherwise} \end{cases}, \\ m_1 &= (g_1 - 1) + (e_1 - 1) \frac{\Gamma_1}{\eta_1}, \\ m_2 &= (g_2 - 1) + (e_2 - 1) \frac{\Gamma_2}{\eta_2}. \end{aligned}$$

Inserting (97),(98) in (96), we get

$$\tilde{W}_2(\mathcal{I}(v_1)) \lesssim \text{TOL}_r^{-2\psi} (\log \text{TOL}_r^{-1})^\varkappa, \quad (99)$$

where

$$\varkappa = \begin{cases} (g_1 - 1) + (e_1 - 1) \frac{\Gamma_1}{\eta_1}, & \Psi = \frac{1+\gamma_1}{1+\gamma_1-w_1+2b_1} \text{ or } \frac{\gamma_2}{\gamma_2-w_2+2b_2} \\ (g_2 - 1) + (e_2 - 1) \frac{\Gamma_2}{\eta_2}, & \Psi = \frac{1+\gamma_1}{\gamma_1-s_1+2b_1} \text{ or } \frac{\gamma_2}{\gamma_2-s_2+2b_2} \end{cases}.$$

Inserting (95) and (99) into (42), we get

$$\mathcal{W}[\mathcal{A}_{\text{MIMC}}(\mathcal{I}(v_1))] \lesssim \text{TOL}_r^{-2-2\varsigma} (\log \text{TOL}_r^{-1})^{2\varrho} + \text{TOL}_r^{-2\Psi} (\log \text{TOL}_r^{-1})^{\varkappa}. \quad (100)$$

To ensure that the first term in (100) dominates the second term, we need to satisfy the condition (60). This concludes the proof.

References

- Juan A Acebrón, Luis L Bonilla, Conrad J Pérez Vicente, Félix Ritort, and Renato Spigler. The Kuramoto model: A simple paradigm for synchronization phenomena. *Reviews of modern physics*, 77(1):137, 2005.
- Hernan P Awad, Peter W Glynn, and Reuven Y Rubinstein. Zero-variance importance sampling estimators for Markov process expectations. *Mathematics of Operations Research*, 38(2):358–388, 2013.
- Mohamed Ben Alaya, Kaouther Hajji, and Ahmed Kebaier. Adaptive importance sampling for multilevel Monte Carlo Euler method. *Stochastics*, 95(2):303–327, 2023.
- Chiheb Ben Hammouda, Nadhir Ben Rached, and Raúl Tempone. Importance sampling for a robust and efficient multilevel Monte Carlo estimator for stochastic reaction networks. *Statistics and Computing*, 30:1665–1689, 2020.
- Nadhir Ben Rached, Abdul-Lateef Haji-Ali, Shyam Mohan Subbiah Pillai, and Raúl Tempone. Double loop importance sampling for McKean-Vlasov stochastic differential equation. *arXiv preprint arXiv:2207.06926*, 2022a.
- Nadhir Ben Rached, Abdul-Lateef Haji-Ali, Shyam Mohan Subbiah Pillai, and Raúl Tempone. Multilevel importance sampling for McKean-Vlasov stochastic differential equation. *arXiv preprint arXiv:2208.03225*, 2022b.
- Mireille Bossy and Denis Talay. Convergence rate for the approximation of the limit law of weakly interacting particles: application to the Burgers equation. *The Annals of Applied Probability*, 6(3):818–861, 1996.
- Mireille Bossy and Denis Talay. A stochastic particle method for the McKean-Vlasov and the Burgers equation. *Mathematics of computation*, 66(217):157–192, 1997.
- Rainer Buckdahn, Juan Li, Shige Peng, and Catherine Rainer. Mean-field stochastic differential equations and associated PDEs. 2017.
- Nick Bush, Ben M Hambly, Helen Haworth, Lei Jin, and Christoph Reisinger. Stochastic evolution equations in portfolio credit modelling. *SIAM Journal on Financial Mathematics*, 2(1):627–664, 2011.

- Nathan Collier, Abdul-Lateef Haji-Ali, Fabio Nobile, Erik Von Schwerin, and Raúl Tempone. A continuation multilevel Monte Carlo algorithm. *BIT Numerical Mathematics*, 55:399–432, 2015.
- Dan Crisan and Eamon McMurray. Smoothing properties of McKean–Vlasov SDEs. *Probability Theory and Related Fields*, 171:97–148, 2018.
- Dan Crisan and Eamon McMurray. Cubature on Wiener space for McKean–Vlasov SDEs with smooth scalar interaction. *The Annals of Applied Probability*, 29(1):130–177, 2019.
- Dan Crisan and Jie Xiong. Approximate McKean–Vlasov representations for a class of SPDEs. *Stochastics An International Journal of Probability and Stochastics Processes*, 82(1):53–68, 2010.
- David Cumin and CP Unsworth. Generalising the Kuramoto model for the study of neuronal synchronisation in the brain. *Physica D: Nonlinear Phenomena*, 226(2):181–196, 2007.
- Ulrich Dobramysl, Sten Rüdiger, and Radek Erban. Particle-based multiscale modeling of calcium puff dynamics. *Multiscale Modeling & Simulation*, 14(3):997–1016, 2016.
- Gonçalo dos Reis, Stefan Engelhardt, and Greig Smith. Simulation of McKean–Vlasov SDEs with super-linear growth. *IMA Journal of Numerical Analysis*, 42(1):874–922, 2022.
- Gonçalo dos Reis, Greig Smith, and Peter Tankov. Importance sampling for McKean-Vlasov SDEs. *Applied Mathematics and Computation*, 453:128078, 2023.
- Radek Erban and Jan Haskovec. From individual to collective behaviour of coupled velocity jump processes: a locust example. *arXiv preprint arXiv:1104.2584*, 2011.
- Wei Fang and Michael B Giles. Multilevel Monte Carlo method for ergodic SDEs without contractivity. *Journal of Mathematical Analysis and Applications*, 476(1):149–176, 2019.
- Derek Michael Forrester. Arrays of coupled chemical oscillators. *Scientific reports*, 5(1):16994, 2015.
- Abdul Lateef Haji Ali. Pedestrian flow in the mean field limit. 2012.
- Abdul-Lateef Haji-Ali and Raúl Tempone. Multilevel and multi-index Monte Carlo methods for the McKean–Vlasov equation. *Statistics and Computing*, 28:923–935, 2018.
- Abdul-Lateef Haji-Ali, Fabio Nobile, and Raúl Tempone. Multi-index Monte Carlo: when sparsity meets sampling. *Numerische Mathematik*, 132:767–806, 2016a.
- Abdul-Lateef Haji-Ali, Fabio Nobile, Erik von Schwerin, and Raúl Tempone. Optimization of mesh hierarchies in multilevel Monte Carlo samplers. *Stochastics and Partial Differential Equations Analysis and Computations*, 4(1):76–112, 2016b.
- Abdul-Lateef Haji-Ali, Håkon Hoel, and Raúl Tempone. A simple approach to proving the existence, uniqueness, and strong and weak convergence rates for a broad class of McKean–Vlasov equations. 2021.

- William RP Hammersley, David Šiška, and Łukasz Szpruch. Weak existence and uniqueness for McKean–Vlasov SDEs with common noise. 2021.
- Carsten Hartmann, Lorenz Richter, Christof Schütte, and Wei Zhang. Variational characterization of free energy: theory and algorithms. *Entropy*, 19(11):626, 2017.
- PD Hinds and MV Tretyakov. Neural variance reduction for stochastic differential equations. *arXiv preprint arXiv:2209.12885*, 2022.
- Ahmed Kebaier and Jérôme Lelong. Coupling importance sampling and multilevel Monte Carlo using sample average approximation. *Methodology and Computing in Applied Probability*, 20:611–641, 2018.
- Dirk P Kroese, Thomas Taimre, and Zdravko I Botev. *Handbook of Monte Carlo methods*. John Wiley & Sons, 2013.
- Yun Li, Xuerong Mao, Qingshuo Song, Fuke Wu, and George Yin. Strong convergence of Euler–Maruyama schemes for McKean–Vlasov stochastic differential equations under local Lipschitz conditions of state variables. *IMA Journal of Numerical Analysis*, 43(2):1001–1035, 2023.
- Henry P McKean Jr. A class of Markov processes associated with nonlinear parabolic equations. *Proceedings of the National Academy of Sciences*, 56(6):1907–1911, 1966.
- S. Méléard. Asymptotic behaviour of some interacting particle systems; McKean–Vlasov and Boltzmann models. In D. Talay and L. Tubaro, editors, *Probabilistic Models for Nonlinear Partial Differential Equations*, volume 1627, pages 42–95. Springer, 1996.
- Grigori N Milstein and Michael V Tretyakov. *Stochastic numerics for mathematical physics*, volume 39. Springer, 2004.
- Yuliya Mishura and Alexander Veretennikov. Existence and uniqueness theorems for solutions of McKean–Vlasov stochastic equations. *Theory of Probability and Mathematical Statistics*, 103:59–101, 2020.
- Nigel J Newton. Variance reduction for simulated diffusions. *SIAM journal on applied mathematics*, 54(6):1780–1805, 1994.
- Alain-Sol Sznitman. Topics in propagation of chaos. *Lecture notes in mathematics*, pages 165–251, 1991.
- Łukasz Szpruch, Shuren Tan, and Alvin Tse. Iterative multilevel particle approximation for McKean–Vlasov SDEs. *The Annals of Applied Probability*, 29(4):2230–2265, 2019.